Accepted Manuscript

Discovery of novel piperidine-substituted indolylarylsulfones as potent HIV NNRTIs via structure-guided scaffold morphing and fragment rearrangement

Xiao Li, Ping Gao, Boshi Huang, Zhongxia Zhou, Zhao Yu, Zheng Yuan, Huiqing Liu, Christophe Pannecouque, Dirk Daelemans, Erik De Clercq, Peng Zhan, Xinyong Liu

PII: S0223-5234(16)30871-6

DOI: 10.1016/j.ejmech.2016.10.009

Reference: EJMECH 8974

To appear in: *European Journal of Medicinal Chemistry*

Received Date: 16 July 2016

Revised Date: 3 October 2016

Accepted Date: 4 October 2016

Please cite this article as: X. Li, P. Gao, B. Huang, Z. Zhou, Z. Yu, Z. Yuan, H. Liu, C. Pannecouque, D. Daelemans, E. De Clercq, P. Zhan, X. Liu, Discovery of novel piperidine-substituted indolylarylsulfones as potent HIV NNRTIs via structure-guided scaffold morphing and fragment rearrangement, *European Journal of Medicinal Chemistry* (2016), doi: 10.1016/j.ejmech.2016.10.009.

Graphical Abstract:

A series of novel indolylarylsulfones (IASs) bearing *N*-substituted piperidine at indole-2-carboxamide were identified as potent HIV NNRTIs by structure-guided scaffold morphing and fragment rearrangement.

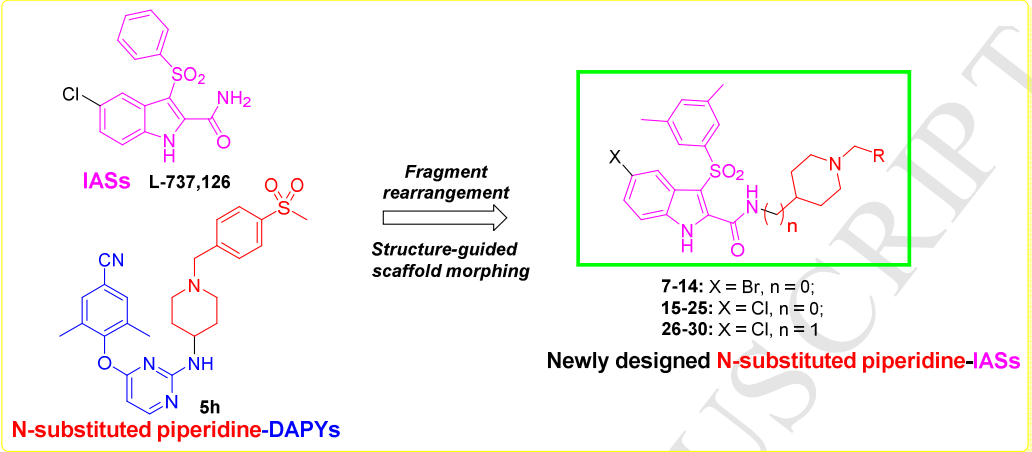

Discovery of Novel Piperidine-substituted Indolylarylsulfones as Potent HIV NNRTIs via Structure-guided Scaffold Morphing and Fragment Rearrangement

Xiao Li[1], Ping Gao[1], Boshi Huang[1], Zhongxia Zhou[1], Zhao Yu[1], Zheng Yuan[3], Huiqing Liu[3], Christophe Pannecouque[2], Dirk Daelemans[2], Erik De Clercq[2], Peng Zhan[1,*], Xinyong Liu[1,*]

[1]*Department of Medicinal Chemistry, Key Laboratory of Chemical Biology (Ministry of Education), School of Pharmaceutical Sciences, Shandong University, 44 West Culture Road, 250012 Jinan, Shandong, P.R. China*

[2]*Rega Institute for Medical Research, KU Leuven, Minderbroedersstraat 10, B-3000 Leuven, Belgium*

[3]*Department of Pharmacology, Shandong University School of Medicine, Shandong University, 44 West Culture Road, 250012 Jinan, Shandong, P.R. China*

Abstract: To further explore the chemical space around the entrance channel of HIV-1 reverse transcriptase (RT), a series of novel indolylarylsulfones (IASs) bearing *N*-substituted piperidine at indole-2-carboxamide were identified as potent HIV NNRTIs by structure-guided scaffold morphing and fragment rearrangement. All the IASs exhibited moderate to excellent potency against wild-type HIV-1 with EC_{50} values ranging from 0.62 μM to 0.006 μM. **8** (EC_{50} = 6 nM) and **18** (EC_{50} = 9 nM) were identified as the most potent compounds, which were more active than NVP and DLV, and reached the same order of EFV and ETV. Furthermore, most compounds maintained high activity agaist various single HIV-1 mutants (L100I, K103N, E138K, Y181C) as well as one double mutant (F227L/V106A) with EC_{50} values in low-micromolar to double-digit nanomolar concentration ranges. Especially, **8** displayed outstanding potency against L100I (EC_{50} = 17 nM with a 2.8-fold resistance ratio) and **18** was relatively more potent to E138K mutant (EC_{50} = 43 nM with a 4.7-fold resistance ratio). Preliminary SARs and molecular modeling studies were also discussed in detail, which may provide valuable insights for further optimization.

*Corresponding authors. Tel: +86 531 88380270; fax: +86 531 88382731; E-mail addresses:zhanpeng1982@sdu.edu.cn & xinyongl@sdu.edu.cn.

Keywords: HIV, NNRTIs, Indolylarylsulfones, Antiviral activity, SAR, Molecular modeling, Chemical space, Drug design.

1. Introduction

Highly active antiretroviral therapy (HAART) in general has significantly changed the progression and outcome of the infection with HIV-1 [1-5]. Non-nucleoside reverse transcriptase inhibitors (NNRTIs) have received a lot of attentions, and have been shown to be a standard component of HAART, because of their favorable potency and low cytotoxicity. So far, five NNRTIs have been approved for AIDS treatment, and about 50 classes of structurally diverse NNRTIs are being widely investigated [6-12]. Over the past few years, considerable efforts have been devoted to the structural modification of diarylpyrimidines (DAPYs), a family of NNRTIs with remarkable anti-HIV-1 activity, leading to the approval of Etravirine (ETV) and Rilpivirine (RPV) (**Figure 1**) as new generation of anti-HIV drugs (approved by US FDA in 2008, 2011, respectively) with significantly improved drug resistance profiles, compared with the first generation NNRTIs [13, 14]. However, hyper sensitivity reactions or other adverse effects have been reported with second-generation NNRTIs [15]. Also, although drug resistance is delayed, it continues to emerge in patients receiving second-generation NNRTIs regimens [16, 17]. Therefore, there is a substantial need for the identification of new inhibitors, especially in additional NNRTIs families, that display a broad spectrum of activity against clinically relevant HIV-1 mutant strains and lower adverse effects [18, 19].

Figure 1

Figure 1. The structures of representative DAPYs (Etravirine, Rilpivirine and **5h**) and IASs (L-737,126 and **7e**), and the newly designed *N*-substituted piperidine-IASs *via* the combination of structure-guided scaffold morphing and fragment rearrangement approaches.

Figure 2

Figure 2. Schematic diagram of the binding modes of IASs and DAPYs with NNIBP: (a) HIV RT in complex with inhibitor **7e** (pink) (PDB code: 2RF2); (b) HIV RT in complex with inhibitor **5h** (dark blue) (PDB code: 3M8Q). These figures were generated using PyMOL (www.pymol.org). Residues important for binding are shown as sticks. Hydrogen bonds are indicated by yellow dashes.

Indolylarylsulfones (IASs), a potent class of NNRTIs developed from the Merck prototype compound L-737,126 (**Figure 1**), have endowed with inhibitory activities against wild-type (WT) and drug-resistant HIV-1 in nanomolar range [20-26]. Based on the crystallography and molecular modeling study (exemplified by **7e**, **Figure 2**), it suggested that the side chain at 2-position of the indole nucleus located into the entrance channel (the protein/solvent interface between the p66 and p51 RT subunits) of NNRTI binding pocket (NNIBP), mainly formed by Leu100, Glu138 and Val179. Additionaly, the groups at this position could build potential hydrogen bonds with around amino acids such as Glu138 [27]. In recent years, to further improve anti-HIV-1 activity and optimize physicochemical properties and pharmacokinetics of IASs, most work on the modification of IASs was focused on introducing different substituents (natural and unnatural amino acids, cyclic and nitrogen containing substituents) into the 2-carboxamide nitrogen by taking advantage of the solvent exposed region, affording derivatives endowed with activities against WT HIV-1 and NNRTI-resistant mutants superior to that of the parent L-737,126 [21-29]. These promising results motivated us to put more efforts in in-depth exploration of untapped chemical space around the entrance channel through chemical modifications at 2-position of indole (**Figure 1**).

The “Pro236 hairpin loop” is another protein/solvent interface in NNIBP that provide broad space that are potentially available to accommodate novel NNRTIs [8]. A systematic exploration of the chemical space around the “Pro236 hairpin loop” led to discovery of novel piperidine-linked aminopyrimidine derivatives with broad activity against WT as well as drug-resistant mutant viruses [30,31]. X-ray crystallographic analysis of early leads showed a water molecule linking the

piperidine nitrogen with the backbone NH of Lys103 (exemplified by **5h**, **Figure 2**). Guided by crystallography and studies in silico, to identify new DAPYs by establishing novel binding interactions with this solvent-accessible region and to further expand the chemical scope of the core ring system in DAPYs families, we made considerable efforts on chemically modification using the privileged *N*-substituted piperidine group, which has given a number of highly active NNRTIs with excellent anti-HIV-1 activity and significantly improved water solubility, which is an urgent issue of existing DAPY drugs [32-44].

In continuation of our research project, inspired by the analyses of this two categories of NNRTIs and based on the concept of "mixed sites inhibitor" [45,46], we planned the structure-based design, synthesis of new IASs characterized by structurally diverse *N*-substituted piperidine groups at the 2-carboxamide to explore the detail of the conformational and space-filling requirements for optimum occupation of the entrance channel (**Figure 1**). Meanwhile, the preferred combination of the 5-halogen-indole core, 3-arylsulfonyl and 2-carboxamide group of original IASs were preserved. Therefore, the present study will highlight the synthesis, biological evaluation of novel IAS derivatives, and the preliminary structure-activity relationships (SARs) and molecular modeling results will also be discussed in detail.

2. Results and Discussion

2.1 Chemistry

To achieve the target compounds **7-30**, the straightforward synthetic route adopted is depicted in **Scheme 1**. Briefly, the commercial available ethyl 5-chloro/bromo-1H-indole-2-carboxylate (**1a** or **1b**) was converted to intermediate **2a** and **2b** by reacting with commercial 3,5-dimethylbenzenethiol in the presence of 1-chloromethyl-4-fluoro-1,4-diazoniabicyclo[2.2.2]octanebis(tetrafluoroborate) (Selettflour^{TM}) [47]. Then treatment of intermediate **2a** or **2b** with *m*-chloroperoxybenzoic acid and lithium hydroxide orderly gave intermediate **4a** or **4b**, which underwent acylation reaction with1-Boc-4-(aminomethyl)-piperidine or 1-Boc-4-amino-piperidine to generate intermediates **5a**, **5b** and **5c** [21-23]. The Boc group of **5a**, **5b** and **5c** was removed in the presence of trifluoroacetic acid (TFA) at

room temperature to afford intermediates **6a**, **6b** and **6c** in good yield [48]. Finally, the target compounds **7-30** was obtained by alkylating at the N atom of piperidine under two different reaction conditions [49]. All the synthesized compounds (displayed in **Table 1**) were confirmed by their spectral data (ESI-MS, ^{1}H NMR and ^{13}C NMR). Spectral data are in accordance with the assumed structures.

Scheme 1.

Scheme 1. Reagents and conditions: (i) 3,5-dimethylbenzenethiol, Selettflour^{TM}, MeCN; (ii) M-chloroperoxybenzoic acid, CH_2Cl_2, 0°C; (iii) LiOH, H_2O, THF, 50°C; (iv) 1-Boc-4-(aminomethyl)-piperidine or 1-Boc-4-aminopiperidine, HATU, EDC·HCl, Et_3N, DMF; (v) CF_3COOH, CH_2Cl_2; (vi) K_2CO_3, DMF, substituted benzyl; (vii) substituted-aldehyde AcOH, $NaBH_3CN$, THF/MeCN.

2.2 Anti-HIV activity evaluation

The newly prepared IAS derivatives were evaluated for their activity against WT HIV-1 strain (IIIB) and HIV-2 strain (ROD) in MT-4 cell cultures using MTT method, respectively. What's more, these compounds were also assayed against frequently encountered single (L100I, K103N, Y181C, Y188L, E138K) or (F227L/V106A, K103N/Y181C (RES056)) double mutant HIV-1 strains for the sake of defining the resistance profiles. The FDA-approved drugs nevirapine (NVP), delavirdine (DLV), efavirenz (EFV) and Etravirine (ETV) were chosen as reference drugs. The biological results are represented as EC_{50} values (anti-HIV activity), CC_{50} values (cytotoxicity) and SI values (selectivity index, given by the CC_{50}/EC_{50} ratio). All the data were illustrated in **Table 1**.

The biological testing results clearly indicated that all the novel IASs exhibited moderate to excellent potency against WT HIV-1 with EC_{50} values in the range of 0.006-0.62 μM and SI values ranging from 93 to 9391. Totally, 18 compounds were much better than those of NVP and reach the same or a higher level of DLV. Thereinto, compounds **8** (EC_{50} = 6 nM, SI = 1005) and **18** (EC_{50} = 9 nM, SI = 1467) were the most active derivatives, which were about 20 and 13 times more active than NVP, 4 and 3 times more active than DLV, respectively, and reached the same order of EFV

and ETV. None of the newly synthesized compounds were active at subtoxic concentration against HIV-2 (ROD), thus the detailed date were not listed.

Against these mutant strains, except for Y188L mutant**,** most compounds maintained high activity against various single mutants with EC_{50} values in low-micromolar to two-digit nanomolar concentration ranges. Notably, **8** displayed outstanding potency against L100I (EC_{50} = 17 nM with a 2.8-fold resistance ratio, namely, $EC_{50(\text{mutant strain})}/EC_{50(\text{WT strain})}$ ratio) and K103N (EC_{50} = 84 nM with a 14-fold resistance ratio) mutant strains, which were more active than the reference drugs NVP, DLV and EFV. More interestingly, compared with **8**, compound **18** bearing a 1,2,4-triazol-3(4H)-one tail displayed different drug resistance profile, which is relatively more potent against E138K mutant (EC_{50} = 43 nM with a 4.7-fold resistance ratio) and L100I mutant HIV-1 strain (EC_{50} = 49 nM with a 5.4-fold resistance ratio), but weak potency against the K103N mutant strain (EC_{50} = 0.18 μM with a 20-fold resistance ratio). Regarding the Y188L mutant, the most sensitive single mutant for IASs, **18** was also found to be the most active one (EC_{50} = 0.84 μM). Besides, fifteen compounds can inhibit F227L/V106A double mutant replication at low-micromolar concentration, while only compound **20** demonstrated remarkable inhibitory activty to K103N/Y181C double mutant (RES056) with EC_{50} value of 4.4 μM.

Based on the analysis of above anti-HIV results, preliminary SARs of these IASs could be delineated as follows (**Figure 3**):

Firstly, we focused on modifications at the terminal groups (R) substituted in the N atom of the piperidine ring. The SAR suggests that the nature of the R substituents have dramatically effects on antiviral activity against WT and mutiple HIV-1 mutant strains. Generally, polar groups substituted benzenes, alkanes or a set of commonly used small heterocycles, with ability to form hydrogen bond, seem to be more favorable at this region, exemplified by **8** (hydroxymethyl) and **18** (1,2,4-triazol-3(4H)-one) as the most two potent compounds. In contrast, some other modifications at this region may lead to a deleterious effect on anti-HIV potency and drug resistance profiles, such as halogene at benzenes **10** (4-Cl, $EC_{50(\text{IIIB})}$ = 0.13 μM), **11** (3-Cl, $EC_{50(\text{IIIB})}$ = 0.30 μM), **23** (4-CF_3, $EC_{50(\text{IIIB})}$ = 0.17 μM), **28** (3-F, $EC_{50(\text{IIIB})}$ =

0.18 μM), cyano-derivatived **29** ($EC_{50(IIIB)}$ = 0.14 μM), and nitro analogue **25** ($EC_{50(IIIB)}$ = 0.62 μM). Moreover, lower cytotoxicities were usually observed in compounds with halo substituents, exemplified by **11** (3-Cl, $CC_{50(IIIB)}$ = 103.0 μM), **10** (4-Cl, $CC_{50(IIIB)}$ = 67.3 μM) and **28** (3-F, $CC_{50(IIIB)}$ = 61.3 μM).

More specifically, for the phenyl-substituted series, amide or sulfamide appeared to be the most favorable groups, closely followed by substituted phenyls in the sequence 3-COMe > 4-Cl > 3-Cl (in **7-14** sub-series); 4-CF_3 > 4-NO_2 (in **15-25** sub-series); 3-F = 3-CN (in **26-30** sub-series). Moreover, the replacement of the substituted phenyls by a set of aromatic heterocycles resulted in comparable level of anti-HIV (WT and mutants) activities, indicating structurally diverse heterocycles, as hydrogen bond donors or receptors, can also better accommodate the chemical environment in this region of RT and have a favorable interactions with surrounding residues. This SAR conclusion is consistent with our design hypothesis.

Interestingly, no substantial difference in antiviral activity against WT and mutant strains can be observed between pyridin-3-yl and pyridin-4-yl counterparts (**12/13**, **16/17**). By contrast, it is noteworthy that thiophene-2-yl (**21**) was always preferred over thiophene-3-yl (**22**) against WT and all the tested mutant strains, especially for L100I, Y181C and F227L/V106A.

Then we focused on substituent effects at 5-position (X substitutions) of indole ring. The results demonstrated that the inhibitory activities (EC_{50} values) against WT HIV-1 seemed only marginally affected by the substitutions (Br or Cl) at the position 5 of the indole nucleus, through the pairwise comparison of the EC_{50} values, namely, **9** (X = Br, $EC_{50(IIIB)}$ = 14 nM) and **19** (X = Cl, $EC_{50(IIIB)}$ = 13 nM); **12** (X = Br, $EC_{50(IIIB)}$ = 19 nM) and **16** (X = Cl, $EC_{50(IIIB)}$ = 12 nM); **13** (X = Br, $EC_{50(IIIB)}$ = 17 nM) and **17** (X = Cl, $EC_{50(IIIB)}$ = 16 nM); **14** (X = Br, $EC_{50(IIIB)}$ = 12 nM) and **20** (X = Cl, $EC_{50(IIIB)}$ = 11 nM). Similarly, in general, the influence on the activity against mutant strains was also negligible.

Lastly, for purpose of exploring the influence of flexibility on anti-HIV activity, piperidine (n = 0) and methylenylpiperidine (n = 1) groups were primarily introduced to indole-2-carboxamide. Piperidine appears to be preferred over

methylenylpiperidine counterpart against WT as well as mutiple mutant HIV-1 strains [e.g. **20** (n = 0, $EC_{50(IIIB)}$ = 11 nM) and **27** (n =1, $EC_{50(IIIB)}$ = 24 nM); **8** (n = 0, $EC_{50\,(IIIB)}$ = 6 nM) and **26** (n = 1, $EC_{50(IIIB)}$ = 32 nM)].

Figure 3.

Figure 3. A illustrative figure of the SARs.

Table1. Activity against HIV-1 strains, cytotoxicity and selectivity indexin MT-4 cells.

Table 1

[a]EC_{50}: concentration of compound required to achieve 50% protection of MT-4 cell cultures against HIV-1-induced cytotoxicity, as determined by the MTT method.

[b]CC_{50}: concentration required to reduce the viability of mock-infected cell cultures by 50%, as determined by the MTT method.

[c]SI: selectivity index, the ratio of CC_{50}/EC_{50}.

Table 1 (Continued). Activity against HIV-1 strains, cytotoxicity and selectivity index in MT-4 cells.

Table 1. (Continued)

2.3 HIV-1 RT inhibition assay

To further confirm that the title compounds target HIV-1 RT, the representative compounds **18** and **30** were selected to be evaluated in recombinant HIV-1 RT inhibitory assays, which use hybrid hybrid poly (A)·oligo $(dT)_{15}$ ($9A_{260}$ nm/mL), lyophilizate as template primer (RT kit, Roche). As shown in **Table 2**, **18** and **30** exhibited moderate inhibition of enzymatic activity with an IC_{50} value of 7.0 μM and 10.1 μM respectively, which is slightly lower than the reference drugs NVP (IC_{50} = 2.8 μM) and ETV (IC_{50} = 1.1 μM). The results further indicated that the newly synthesized IAS derivatives, represented by **18** and **30**, do indeed act as typical HIV-1 NNRTIs.

It is noteworthy that the high and low order of the enzyme-inhibitory potencies in this study was inconsistent with that of their antiviral activities to some extent (**18**, **30**

& NVP). These differences usually ascribed to template-specific variation in the relationship between polymerase processivity and HIV-RT-RNA binding affinity, which have been observed in other NNRTI families [50]. Besides, compared with NVP, these piperidine-substituted IASs have multiple hydrogen bond donor and acceptor sites, there is a high probability of formation of cocrystals or salts. Therefore, the differences between the two assay systems can be attributed at least in part to differences in the physiochemical properties (especially the intrinsic solubility).

Table 2. Inhibitory activity of compounds**18**, **30**, NVP and ETV against HIV-1 RT.

Table 2.

[a]IC_{50}: inhibitory concentration of test compound required to inhibit biotin deoxyuridine triphosphate (biotin-dUTP) incorporation into HIV-1 (WT) RT by 50%.

2.4. Molecular modeling analysis

With the aim to shed light on the preferred binding mode in the NNIBP and rationalize SARs results of novel IASs, molecular modeling of the most potent compounds **8** and **18** were performed by using software Surflex-Dock moduleo Sybyl-X 1.1 [51] and the docking results were shown by PyMOL 1.5.

The theoretical binding mode of compounds **8** and **18** to the NNIBP is shown in **Figure 4**. The similar binding mode as previously reported IASs can be observed and notable features can be summarized as follows: (i) The 3,5-dimethylphenyl moiety fitted into an aromatic-rich binding subpocket formed by side chains of Tyr181, Tyr188 and Trp229, exhibiting crucial hydrophobic interactions. (ii) Double hydrogen bonds were formed between the indole NH and the carbonyl oxygen of Lys101, remarkablely improving the stability of RT-inhibitor complex. (iii) The chlorine or bromine atom at the position 5 of indole was very closed to Val106 and probably established halogen bond interactions.

From analysis of the results, the piperidine moiety could well occupy the entrance channel of NNIBP and the substituent on it (the triazolone moiety of compound **18**) located toward the protein/solvent interface (**Figure 4c**). Specifically, extra H-bond interaction was built between the nitrogen atom of the triazolone and

Glu138, which is important in the binding of this compound (**Figure 4b**).

Overall, the molecular modeling analysis confirmed our the initial design assumption that introducing a *N*-substituted piperidine at indole-2-carboxamide of IASs could not only make terminal substituent of new compounds to extend more closer to the protein/solvent interface of HIV-1 RT, but also built potential interactions with surrounding residues (especially Glu138). These preliminary conclusions will be taken into account for the next round rational structural optimization.

Figure 4.

Figure 4. Predicted binding modes of novel IASs in the allosteric site of HIV-1 WT RT (PDB code: 2rf2): (a) Ribbon model of the **8** binding; (b) Ribbon model of the **18** binding (c) Surface presentation of **18** located toward a solvent exposure region. Hydrogen bonds are indicated with dashed lines in red, and hydrogen atoms are omitted for clarity.

3. Conclusion

In summary, to explore the uncharted chemical space around the entrance channel in RT, a series of novel IASs bearing *N*-substituted piperidine at indole-2-carboxamide were identified as potent HIV NNRTIs by the structure-based scaffold morphing and fragment rearrangement approaches. All the novel IASs exhibited moderate to excellent potency against WT HIV-1 in MT-4 cells. Especially, compounds **8** and **18** were identified as the most promising leads with EC_{50} value of 6 nM and 9 nM, respectively, which were more active than NVP and DLV, and reached the same order of EFV and ETV. Furthermore, most compounds maintained high activity against various single mutants as well as F227L/V106A double mutant with EC_{50} values in low-micromolar to double-digit nanomolar concentration range. Preliminary SARs based on anti-HIV-1 activities were also discussed in detail and molecular modelin*g* studies were carried out to investigate the interactions between IASs and HIV-1 RT. Taking full advantage of these valuable information, further efforts to improve drug resistance profile of these IAS derivatives is underway in our laboratory and will be reported in due course.

4. Experimental Section

4.1. Synthetic procedures and analytical data

Mass spectrometry was performed on an API 4000 triple-quadrupole mass spectrometer (Applied Biosystems/MDS Sciex, Concord, ON, Canada). ^{1}H-NMR and ^{13}C-NMR spectra were recorded on a Bruker AV-400 spectrometer (Bruker BioSpin, Switzerland), using solvents as indicated (DMSO-d_6). Chemical shifts were reported in δ values (ppm) with tetramethylsilane as the internal reference, and J values were reported in hertz (Hz). Melting points (mp) were determined on a micromelting point apparatus (Tian Jin Analytical Instrument Factory, Nankai, Tianjin, China). Flash column chromatography was performed on columns packed with silica gel 60 (200–300 mesh) (Qingdao waves silica gel desiccant co., Ltd, Qingdao, China). Thin layer chromatography was performed on pre-coated HUANGHAI® HSGF254, 0.15-0.2 mm TLC-plates (Yantai Jiangyou Silica Gel Development Co., Ltd., Yantai, Shandong, China).

*4.1.1 General procedure for the synthesis of 5-chloro-3-(3,5-dimethylphenyl-sulfonyl)-1H-indole-2-carboxylic acid (**6a**)*

Ethyl 5-bromo-3-(3,5-dimethylphenylthio)-1H-indole-2-carboxylate(**2a**): To a solution of ethyl 5-bromo-1H-indole-2-carboxylate (**1a**, 0.10 g, 0.373 mmol) in MeCN (10 mL) at ambient temperature was successively added 3,5-dimethylbenzenethiol (51.6 mg, 0.373 mmol, 50 μL) and 1-chloromethyl-4-fluoro-1,4-diazoniabicyclo[2.2.2]octane bis(tetrafluoroborate) (0.10 g, 0.373 mmol) and the resulting mixture was stirred for 6 h (monitored by TLC). The solvent was removed under reduced pressure and water (30 mL) was added and extracted with CH_2Cl_2 (3×10 mL). Combined organic phase was washed with brine, dried over anhydrous $MgSO_4$, filtered and concentrated. Purification on silica gel (ethyl acetate: petroleum (EA:PE) = 1:8) gave **2a** as a white solid. Yield: 50%.

Ethyl 5-bromo-3-(3,5-dimethylphenylsulfonyl)-1H-indole-2-carboxylate (**3a**): 3-Chloroperoxybenzoic acid (0.128 g, 0.742 mmol) was added to an ice-cooled solution of crude intermediate **2a** (0.10 g, 0.247 mmol) in anhydrous CH_2Cl_2. The

reaction mixture was stirred at room temperature for 3 h, then poured on crushed ice, and extracted with CH_2Cl_2 (3×10 mL). The organic phase was shaken with saturated solution of sodium hydrogen carbonate and then brine, dried over anhydrous $MgSO_4$, filtered and concentrated under reduced pressure. The obtained crude product was recrystallized using EA to give the pure compound **3a** as a white solid. Yield: 68.8%, mp: 205-207 °C. ESI-MS: m/z 436.3 (M+1). $C_{19}H_{18}BrNO_4S$ [435.01].

5-Bromo-3-(3,5-dimethylphenylsulfonyl)-1H-indole-2-carboxylic acid (**4a**): Crude intermediate **3a** (0.10 g, 0.229 mmol) was dissolved in the THF-H_2O mixture (6 mL/6 mL) at room temperature followed by addition of lithium hydroxide (16.5 mg, 0.687 mmol). The reaction mixture was stirred at 50 °C for 24 hours (monitored by TLC), then the THF was removed under reduced pressure. The residue was diluted with water and modulated to pH 5-6 by adding diluted hydrochloric acid. The precipitated compound **4a** was filtered by suction filtration and air-dried to a white powder. Yield: 66.5%, mp: 215-217 °C. ESI-MS: m/z 425.3 (M+18). $C_{17}H_{14}BrNO_4S$ [406.98].

tert-Butyl-4-(5-bromo-3-(3,5-dimethylphenylsulfonyl)-1H-indole-2-carboxamido)piperidine-1-carboxylate (**5a**): The reaction mixture of intermediate **4a** (1.0 g, 2.45 mmol), HATU (1.39 g, 3.67 mmol), 4-amino-1-Boc-piperidine (0.735 g, 3.67 mmol) and *N*,*N*-diisopropylethyl-amine (0.949 g, 7.35 mmol, 1.3 mL) in 10 mL DMF was stirred at ambient temperature for 24 h. After removal of the solvent under reduced pressure, the residues was redissolved in THF (100 mL) and washed with saturated sodium hydroxide aqueous solution. Then organic phase was dried over anhydrous $MgSO_4$, filtered and concentrated. Purification on silica gel (EA:PE = 1:4) gave **5a** as a white solid. Yield: 47.5%.

5-Chloro-3-(3,5-dimethylphenyl-sulfonyl)-1H-indole-2-carboxylic acid (**6a**): Trifluoroacetic acid (1 mL) was added dropwise under stirring to a solution of intermediate **5a** (0.5 g, 0.848 mmol) in CH_2Cl_2 (2 mL) at room temperature and stirred for 4 h. To the reaction mixture was added water and neutralized with 2 N NaOH to pH 8, and the organic layer was separated and dried over anhydrous $MgSO_4$, filtered and concentrated under reduced pressure to give the product **6a** as white solid.

Yield: 75.4%, mp: 230-231 ℃. ESI-MS: m/z 490.4 (M+1). $C_{22}H_{24}BrN_3O_3S$ [489.07].

*4.1.2 General procedure for the synthesis of 5-chloro-3-(3,5-dimethylphenyl-sulfonyl)-N-(piperidin-4-yl)-1H-indole-2-carboxamide (**6b**)*

Using starting material ethyl 5-chloro-1H-indole-2-carboxylate and following the procedure as in the preparation of **6a** to give **6b**.

Ethyl 5-chloro-3-(3,5-dimethylphenylthio)-1H-indole-2-carboxylate (**2b**): Yield: 58.4%, mp: 135-136℃. ESI-MS: m/z 360.4 (M+1), 377.5 (M+18), 382.4 (M+23). $C_{19}H_{18}ClNO_2S$ [359.07].

Ethyl 5-chloro-3-(3,5-dimethylphenylsulfonyl)-1H-indole-2-carboxylate (**3b**): Yield: 58.8%, mp: 210-211 ℃. ESI-MS: m/z 392.0706 (M+1). $C_{19}H_{18}ClNO_4S$ [391.06].

5-Chloro-3-(3,5-dimethylphenylsulfonyl)-1H-indole-2-carboxylic acid (**4b**): Yield: 65.8%, mp: 270 ℃, decomposition. ESI-MS: m/z 386.5 (M+1). $C_{17}H_{14}ClNO_4S$ [363.03].

tert-Butyl-4-(5-chloro-3-(3,5-dimethylphenylsulfonyl)-1H-indole-2-carboxamido)piperidine-1-carboxylate (**5b**): Yield: 52.2%, mp: 240-242 ℃. ESI-MS: m/z 545.14 (M+1), 563.4 (M+18). $C_{27}H_{32}ClN_3O_5S$ [545.18].

5-Chloro-3-(3,5-dimethylphenylsulfonyl)-N-(piperidin-4-yl)-1H-indole-2-carbox amide (**6b**): Yield: 70.1%, mp: 235-236 ℃. ESI-MS: m/z 446.3 (M+1). $C_{22}H_{24}ClN_3O_3S$ [445.12].

*4.1.3 General procedure for the synthesis of5-chloro-3-(3,5-dimethylphenyl-sulfonyl)-N-(piperidin-4-ylmethyl)-1H-indole-2-carboxamide (**6c**)*

Using intermediate **4b** and 1-Boc-4-aminomethylpiperidineand following the procedure as in the preparation of **6b** to give **6c**.

tert-Butyl-4-((5-chloro-3-(3,5-dimethylphenylsulfonyl)-1H-indole-2-carboxamid o)methyl)piperidine-1-carboxylate (**5c**): Yield: 48.2%, mp: 246-248 ℃.

5-Chloro-3-(3,5-dimethylphenylsulfonyl)-*N*-(piperidin-4-ylmethyl)-1H-indole-2-carboxamide (**6c**): Yield: 76.3%, mp: 239-241 ℃. ESI-MS: m/z 460.3(M+1). $C_{23}H_{26}ClN_3O_3S$ [459.14].

*4.1.4 General procedure for the synthesis of target compounds (**7-20**, **26-30**)*

Intermedite **6a**, **6b** or **6c** (0.65mmol, 1 equiv), K_2CO_3 (0.10 g, 0.76 mmol, 1.2 equiv), and different appropriate RCH_2X (X = Cl, Br) (1.1 equiv) were dissolved in DMF (10 mL). The reaction mixture was stirred at ambient temperature for 4 hours and then evaporated under reduced pressure. Water (30 mL) was added and extracted with EA (3×10 mL). Combined organic phase was washed with brine, dried over anhydrous $MgSO_4$, filtered and concentrated. The residue was purified on silica gel using EA-PE system and pure fractions were collected, concentrated and recrystallized, giving the desired compounds (**7-20**, **26-30**).

*4.1.5.N-(1-(3-Methoxybenzyl)piperidin-4-yl)-5-bromo-3-(3,5-dimethylphenyl-sulfonyl)-1H-indole-2-carboxamide (**7**)*

White solid, yield: 43.2%. mp: 175-177 °C. ^{1}H NMR (400MHz, DMSO-d_6, ppm)δ: 13.02 (s, 1H, indole-NH), 8.95 (s, 1H, CONH), 8.09 (s, 1H, indole-H), 7.62 (s, 2H, Ph-H), 7.50 (q, 2H, *J* = 8.00 Hz, indole-H), 7.26 (t, 2H, *J* = 8.00 Hz, Ph'-H), 6.88 (s, 2H, Ph'-H), 6.83 (d, 1H, *J* = 8.00 Hz, Ph-H), 3.86 (s, 1H, piperidine-H), 3.73 (s, 3H, OCH_3), 3.46 (s, 2H, benzyl-CH_2), 2.79 (s, 2H, piperidine-H), 2.31 (s, 6H, 2×CH_3), 2.14 (s, 2H, piperidine-H), 1.93 (s, 2H, piperidine-H), 1.59 (s, 2H, piperidine-H). ^{13}C NMR (100MHz, DMSO-d_6, ppm) δ: 159.73 (C=O), 158.99, 143.05, 140.74, 139.43 (2×C), 137.73, 135.14, 133.58, 129.67, 127.60, 126.34, 124.10 (2×C), 122.36, 121.34, 115.70 (2×C), 114.58, 112.74, 111.53, 62.49 (CH_2), 55.40 (2×CH_2), 52.07(O-CH_3), 47.28, 31.65 (2×CH_2), 21.24 (2×CH_3). ESI-MS: m/z 610.3 (M+1). $C_{30}H_{32}BrN_3O_4S$ [609.13].

*4.1.6. 5-Bromo-3-(3,5-dimethylphenylsulfonyl)-N-(1-(2-hydroxyethyl)piperidin-4-yl) -1H-indole-2-carboxamide (**8**)*

White solid, yield: 40.1%. mp: 220-222 °C. ^{1}H NMR (400MHz, DMSO-d_6, ppm) δ: 13.20-12.59 (b, 1H, indole-NH), 8.95 (d, 1H, *J* = 8.00 Hz, CONH), 8.08 (s, 1H, Indole-H), 7.63 (s, 2H, Ph-H), 7.50 (q, 2H, *J* = 8.00 Hz, Indole-H), 7.26 (s, 1H, Ph-H), 4.44(s, 1H, OH), 3.86 (s, 1H, piperidine-H), 3.34 (s, 2H, CH_2), 2.91 (s, 2H, piperidine-H), 2.45 (s, 2H, CH_2), 2.31 (s, 6H, 2×CH_3), 2.22 (s, 2H, piperidine-H),

1.91 (s, 2H, piperidine-H), 1.60 (s, 2H, piperidine-H). ^{13}C NMR (100MHz, DMSO-d_6, ppm) δ: 159.08 (C=O), 143.10, 139.41(2×C), 137.89, 135.11, 133.66, 127.53, 126.34, 124.11 (2×C), 122.33, 115.73, 115.65, 111.49, 60.59 (CH_2), 58.98 (CH_2), 52.54 (2×CH_2), 47.13, 31.47 (2×CH_2), 21.25 (2×CH_3). HRMS: m/z 536.1040 (M+3). $C_{24}H_{28}BrN_3O_4S$ [533.1].

*4.1.7. N-(1-(4-Sulfonamido-benzyl)piperidin-4-yl)-5-bromo-3-(3,5-dimethylphenyl-sulfonyl)-1H-indole-2-carboxamide (**9**)*

White solid, yield: 42.1%. mp: 170-171 °C. ^{1}H NMR (40 0MHz, DMSO-d_6, ppm) δ: 13.01 (s, 1H, indole-NH), 8.97 (s, 1H, CONH), 8.09 (s, 1H, indole-H), 7.80 (d, 2H, *J* = 8.00 Hz, Ph'-H), 7.62 (s, 2H, Ph-H), 7.51-7.44 (m, 4H, indole-H, Ph'-H), 7.32 (s, 2H, $SONH_2$), 7.27 (s, 1H, Ph-H), 3.87 (s, 1H, piperidine-H), 3.56 (s, 2H, benzyl-CH_2), 2.81 (d, 2H, *J* = 12.00 Hz, piperidine-H), 2.31 (s, 6H, 2×CH_3), 2.20 (t, 2H, *J* = 12.00 Hz, piperidine-H), 1.93 (d, 2H, *J* = 8.00 Hz, piperidine-H), 1.63 (q, 2H, *J* = 12.00 Hz, piperidine-H). ^{13}C NMR (100MHz, DMSO-d_6, ppm) δ: 158.99 (C=O), 143.39, 143.20, 143.03, 139.44 (2×C), 137.70, 135.16, 133.54, 129.41 (2×C), 127.63, 126.30, 126.11 (2×C), 124.10 (2×C), 122.36, 115.71, 115.69, 111.55, 61.88 (CH_2), 52.10 (2×CH_2), 47.23 (CH), 31.65 (2×CH_2), 21.25 (2×CH_3). ESI-MS: m/z 659.4 (M+1). $C_{29}H_{31}BrN_4O_5S_2$ [658.09].

*4.1.8.N-(1-(4-Chlorobenzyl)piperidin-4-yl)-5-bromo-3-(3,5-dimethylphenylsulfonyl)-1 H-indole-2-carboxamide (**10**)*

White solid, yield: 46.2%. mp: 229-230 °C. ^{1}H NMR (400MHz, DMSO-d_6, ppm) δ: 13.07-12.94 (br, 1H, indole-NH), 8.97 (d, 1H, *J* = 8.00 Hz, CONH), 8.09 (s, 1H, indole-H), 7.62 (s, 2H, Ph-H), 7.50 (q, 2H, *J* = 8.00 Hz, indole-H), 7.30 (d, 2H, *J* = 8.00 Hz, Ph'-H), 7.35 (d, 2H, *J* = 8.00 Hz, Ph'-H), 7.26 (s, 1H, Ph-H), 3.86 (s, 1H, piperidine-H), 3.48 (s, 2H, benzyl-CH_2), 2.80 (d, 2H, *J* = 12.00 Hz, piperidine-H), 2.31 (s, 6H, 2×CH_3), 2.17 (t, 2H, *J* = 12.00 Hz, piperidine-H), 1.93 (d, 2H, *J* = 12.00 Hz, piperidine-H), 1.61 (q, 2H, *J* = 12.00 Hz, piperidine-H). ^{13}C NMR (100MHz, DMSO-d_6, ppm) δ: 158.99 (C=O), 143.02, 139.43 (2×C), 138.12, 137.71, 135.15, 133.54, 131.84, 130.93 (2×C), 128.62 (2×C), 127.62, 126.29, 124.10 (2×C), 122.35, 115.71, 115.68, 111.55, 61.60 (CH_2), 51.99 (2×CH_2), 47.24 (CH), 31.64 (2×CH_2),

21.24 (2×CH_3). HRMS: m/z 615.1481 (M+1). $C_{29}H_{29}BrClN_3O_3S$ [613.08].

*4.1.9.N-(1-(3-Cyanobenzyl)piperidin-4-yl)-5-bromo-3-(3,5-dimethylphenylsulfonyl)-1H-indole-2-carboxamide (**11**)*

White solid, yield: 42.3%. mp: 223-236 °C. ^{1}H NMR (400MHz, DMSO-d_6, ppm) δ: 13.03 (s, 1H, indole-NH), 8.97 (d, 1H, *J* = 8.00 Hz, CONH), 8.09 (s, 1H, indole-H), 7.76 (d, 2H, *J* = 12.00 Hz, Ph'-H), 7.69 (d, 1H, *J* = 8.00 Hz, Ph'-H), 7.63 (s, 2H, Ph-H), 7.58 (t, 1H, *J* = 8.00 Hz, Ph'-H), 7.50 (q, 2H, *J* = 8.00 Hz, indole-H), 7.26 (s, 1H, Ph-H), 3.87 (s, 1H, piperidine-H), 3.56 (s, 2H, benzyl-CH_2), 2.81 (d, 2H, *J* = 12.00 Hz, piperidine-H), 2.31 (s, 6H, 2×CH_3), 2.21 (t, 2H, *J* = 12.00 Hz, piperidine-H), 1.94 (d, 2H, *J* = 12.00 Hz, piperidine-H), 1.63 (q, 2H, *J* = 12.00 Hz, piperidine-H). ^{13}C NMR (100MHz, DMSO-d_6, ppm) δ: 158.98 (C=O), 143.01, 139.43 (2×C), 137.67, 135.16, 134.05, 133.58, 133.52, 132.48, 131.28, 129.95, 127.64, 126.29, 124.11 (2×C), 122.36, 119.38, 115.72, 115.67, 111.69, 111.57, 61.36 (CH_2), 51.95 (2×CH_2), 47.18 (CH), 31.61 (2×CH_2), 21.24 (2×CH_3). ESI-MS: m/z 605.4 (M+1). $C_{30}H_{29}BrN_4O_3S$ [604.11].

*4.1.10.5-Bromo-3-(3,5-dimethylphenylsulfonyl)-N-(1-(pyridin-3-ylmethyl)piperidin-4-yl)-1H-indole-2-carboxamide (**12**)*

White solid, yield: 47.8%. mp: 220-221 °C. ^{1}H NMR (400MHz, DMSO-d_6, ppm)δ: 13.02 (s, 1H, indole-NH), 8.97 (d, 1H, *J* = 8.00 Hz, CONH), 8.51 (s, 1H, pyridine-H), 8.48 (d, 1H, *J* = 4.00 Hz, pyridine-H), 8.09 (s, 1H, indole-H), 8.48 (d, 1H, *J* = 8.00 Hz, pyridine-H), 7.63 (s, 2H, Ph-H), 7.50 (q, 2H, *J* = 8.00 Hz, indole-H), 7.38 (dd, 1H, J_1 = 8.00 Hz, J_2 = 4.00 Hz, pyridine-H), 7.26 (s, 1H, Ph-H), 3.86 (s, 1H, piperidine-H), 3.52 (s, 2H, benzyl-CH_2), 2.81 (d, 2H, *J* = 12.00 Hz, piperidine-H), 2.31 (s, 6H, 2×CH_3), 2.19 (t, 2H, *J* = 12.00 Hz, piperidine-H), 1.93 (d, 2H, *J* = 12.00 Hz, piperidine-H), 1.61 (q, 2H, *J* = 12.00 Hz, piperidine-H). ^{13}C NMR (100MHz, DMSO-d_6, ppm) δ: 159.01 (C=O), 150.43, 148.74, 143.02, 139.42 (2×C), 137.73, 136.90, 135.14, 134.38, 133.54, 127.61, 126.28, 124.11 (2×C), 123.90, 122.35, 115.70, 115.68, 111.55, 59.67 (CH_2), 51.97 (2×CH_2), 47.22 (CH), 31.62 (2×CH_2), 21.24 (2×CH_3). ESI-MS: m/z 581.1 (M+1). $C_{28}H_{29}BrN_4O_3S$ [580.11].

4.1.11.5-Bromo-3-(3,5-dimethylphenylsulfonyl)-N-(1-(pyridin-4-ylmethyl)piperidin-4-

*yl)-1H-indole-2-carboxamide (**13**)*

White solid, yield: 46.6%. mp: 243-244 °C.^{1}H NMR (400MHz, DMSO-d_6, ppm)δ: 13.03 (s, 1H, Indole-NH), 8.98 (d, 1H, *J* = 8.00 Hz, CONH), 8.53(d, 2H, *J* = 4.00 Hz, pyridine-H), 8.09 (s, 1H, Indole-H), 7.63 (s, 2H, Ph-H), 7.50 (q, 2H, *J* = 8.00 Hz, Indole-H), 7.35 (d, 2H, *J* = 8.00 Hz, pyridine-H), 7.27 (s, 1H, Ph-H), 3.88 (s, 1H, piperidine-H), 3.53 (s, 2H, benzyl-CH_2), 2.81 (d, 2H, *J* = 12.00 Hz, piperidine-H), 2.31 (s, 6H, 2×CH_3), 2.21 (t, 2H, *J* = 8.00 Hz, piperidine-H), 1.94 (d, 2H, *J* = 8.00 Hz, piperidine-H), 1.61 (q, 2H, *J* = 8.00 Hz, piperidine-H). ^{13}C NMR (100MHz, DMSO-d_6, ppm) δ: 159.01 (C=O), 150.02 (2×C), 148.27, 143.01, 139.43 (2×C), 137.70, 135.16, 133.52, 127.64, 126.27, 124.11 (4×C), 122.35, 115.72, 115.67, 111.57, 61.15 (CH_2), 52.13 (2×CH_2), 47.14 (CH), 31.60 (2×CH_2), 21.14 (2×CH_3). ESI-MS: m/z 581.3 (M+1). $C_{28}H_{29}BrN_4O_3S$ [580.11].

*4.1.12.N-(1-(4-Carbamoylbenzyl)piperidin-4-yl)-5-bromo-3-(3,5-dimethylphenyl-sulfonyl)-1H-indole-2-carboxamide (**14**)*

White solid, yield: 48.1%. mp: 175-176 °C. ^{1}H NMR (400MHz, DMSO-d_6, ppm) δ: 13.02 (s, 1H, indole-NH), 8.97 (d, 1H, *J* = 8.00 Hz, CONH), 8.09 (s, 1H, indole-H), 7.94 (s, 1H, NH_2), 7.86 (d, 2H, *J* = 8.00 Hz, Ph'-H), 7.63 (s, 2H, Ph-H), 7.50 (q, 2H, *J* = 8.00 Hz, indole-H), 7.40 (d, 2H, *J* = 8.00 Hz, Ph'-H), 7.33 (s, 1H, NH_2), 7.27 (s, 1H, Ph-H), 3.86 (s, 1H, piperidine-H), 3.54 (s, 2H, benzyl-CH_2), 2.81 (d, 2H, *J* = 12.00 Hz, piperidine-H), 2.31 (s, 6H, 2×CH_3), 2.18 (t, 2H, *J* = 8.00 Hz, piperidine-H), 1.93 (d, 2H, *J* = 8.00 Hz, piperidine-H), 1.62 (q, 2H, *J* = 8.00 Hz, piperidine-H). ^{13}C NMR (100MHz, DMSO-d_6, ppm) δ: 168.23 (C=O), 158.99 (C=O), 143.02, 142.50, 139.43 (2×C), 137.71, 135.15, 133.53, 133.46, 128.86 (2×C), 127.93 (2×C), 127.62, 126.29, 124.11 (2×C), 122.36, 115.71, 115.68, 111.55, 60.23 (CH_2), 52.09 (2×CH_2), 47.25 (CH), 31.65 (2×CH_2), 21.24 (2×CH_3). HRMS: m/z 625.1344 (M+3). $C_{30}H_{31}BrN_4O_4S$ [622.12].

*4.1.13.N-(1-(4-(Methylsulfonyl)benzyl)piperidin-4-yl)-5-chloro-3-(3,5-dimethylphenyl sulfonyl)-1H-indole-2-carboxamide (**15**)*

White solid, yield: 55.1%. mp: 179-180 °C. ^{1}H NMR (400MHz, DMSO-d_6, ppm)δ: 13.01 (s, 1H, indole-NH), 8.98 (d, 1H, *J* = 8.00 Hz, CONH), 7.94 (s, 1H,

indole-H), 7.91(d, 2H, *J* = 8.00 Hz, Ph'-H), 7.63 (s, 2H, Ph-H), 7.61(d, 2H, *J* = 8.00 Hz, Ph'-H), 7.55 (d, 1H, *J* = 8.00 Hz, indole-H), 7.56 (d, 1H, *J* = 8.00 Hz, indole-H), 7.26 (s, 1H, Ph-H), 3.87 (s, 1H, piperidine-H), 3.61 (s, 2H, benzyl-CH_2), 3.21 (s, 2H, SO_2CH_3), 2.81 (d, 2H, *J* = 8.00 Hz, piperidine-H), 2.31 (s, 6H, 2×CH_3), 2.22 (t, 2H, *J* = 12.00 Hz, piperidine-H), 1.94 (d, 2H, *J* = 8.00 Hz, piperidine-H), 1.61 (q, 2H, *J* = 12.00 Hz, piperidine-H). ^{13}C NMR (100MHz, DMSO-d_6, ppm) δ: 159.03(C=O), 145.49, 143.04, 139.86, 139.44 (2×C), 137.87, 135.15, 133.29, 129.76 (2×C), 127.68, 127.43 (2×C), 125.71, 125.10, 124.12 (2×C), 119.34, 115.33, 111.72, 61.80 (CH_2), 52.11 (2×CH_2), 47.19 (CH), 44.08 (CH_3), 31.65 (2×CH_2), 21.25 (2×CH_3). ESI-MS: m/z 614.3.4 (M+1). $C_{30}H_{32}ClN_3O_5S_2$ [613.15].

*4.1.14.5-Chloro-3-(3,5-dimethylphenylsulfonyl)-N-(1-(pyridin-3-ylmethyl)piperidin-4-yl)-1H-indole-2-carboxamide (**16**)*

White solid, yield: 50.0%. mp: 224-225 °C. ^{1}H NMR (400MHz, DMSO-d_6, ppm)δ: 13.01 (s, 1H, Indole-NH), 8.97 (d, 1H, *J* = 8.00 Hz, CONH), 8.51 (s, 1H, pyridine-H), 8.48 (d, 1H, *J* = 4.00 Hz, pyridine-H), 7.95 (s, 1H, indole-H), 7.73 (d, 1H, *J* = 8.00 Hz, pyridine-H), 7.63 (s, 2H, Ph-H), 7.55 (d, 1H, *J* = 8.00 Hz, pyridine-H), 7.38 (q, 2H, *J* = 8.00 Hz, indole-H), 7.26 (s, 1H, Ph-H), 3.86 (s, 1H, piperidine-H), 3.53 (s, 2H, benzyl-CH_2), 2.81 (d, 2H, *J* = 8.00 Hz, piperidine-H), 2.31 (s, 6H, 2×CH_3), 2.19 (t, 2H, *J* = 8.00 Hz, piperidine-H), 1.93 (d, 2H, *J* = 8.00 Hz, piperidine-H), 1.62 (q, 2H, *J* = 12.00 Hz, piperidine-H). ^{13}C NMR (100MHz, DMSO-d_6, ppm) δ: 159.02 (C=O), 150.43, 148.74, 143.04, 139.42 (2×C), 137.87, 136.90, 135.14, 134.39, 133.29, 127.68, 125.71, 125.09, 124.12 (2×C), 123.89, 119.35, 115.33, 111.73, 59.67 (CH_2), 51.97 (2×CH_2), 47.22 (CH), 31.62 (2×CH_2), 21.24 (2×CH_3). ESI-MS: m/z 537.4 (M+1) . $C_{28}H_{29}ClN_4O_3S$ [536.16].

*4.1.15.5-Chloro-3-(3,5-dimethylphenylsulfonyl)-N-(1-(pyridin-4-ylmethyl)piperidin-4-yl)-1H-indole-2-carboxamide (**17**)*

White solid, yield: 50.5%. mp: 240-241 °C. ^{1}H NMR (400MHz, DMSO-d_6, ppm)δ: 13.02 (s, 1H, indole-NH), 8.98 (d, 1H, *J* = 8.00 Hz, CONH), 8.52 (d, 2H, *J* = 4.00 Hz, pyridine-H) 7.95 (s, 1H, indole-H), 7.63 (s, 2H, Ph-H), 7.55 (d, 1H, *J* = 8.00 Hz, indole-H), 7.35 (d, 3H, *J* = 8.00 Hz, indole-H, pyridine-H), 7.26 (s, 1H, Ph-H),

3.87 (s, 1H, piperidine-H), 3.53 (s, 2H, benzyl-CH_2), 2.81 (d, 2H, *J* = 12.00 Hz, piperidine-H), 2.31 (s, 6H, 2×CH_3), 2.22 (t, 2H, *J* = 12.00 Hz, piperidine-H), 1.93 (d, 2H, *J* = 12.00 Hz, piperidine-H), 1.62 (q, 2H, *J* = 12.00 Hz, piperidine-H).^{13}C NMR (100MHz, DMSO-d_6, ppm) δ: 159.03 (C=O), 150.02 (2×C), 148.26, 143.03, 139.43 (2×C), 137.85, 135.15, 133.28, 127.69, 125.71, 125.11, 124.12 (2×C), 124.09 (2×C), 119.55, 115.33, 111.74, 61.16 (CH_2), 52.13 (2×CH_2), 47.15 (CH), 31.62 (2×CH_2), 21.24 (2×CH_3). ESI-MS: m/z 537.6 (M+1) . $C_{28}H_{29}ClN_4O_3S$ [536.16].

*4.1.16.5-Chloro-3-(3,5-dimethylphenylsulfonyl)-N-(1-((4-methyl-5-oxo-4,5-dihydro-1 H-1,2,4-triazol-3-yl)methyl)piperidin-4-yl)-1H-indole-2-carboxamide (**18**)*

White solid, yield: 53.1%. mp: 274-275 °C. ^{1}H NMR (400MHz, DMSO-d_6, ppm) δ: 13.02 (s, 1H, indole-NH), 11.52 (s, 1H, triazole-NH), 8.95 (d, 1H, *J* = 8.00 Hz, CONH), 7.94 (s, 1H, indole-H), 7.63 (s, 2H, Ph-H), 7.55 (d, 1H, *J* = 8.00 Hz, indole-H), 7.36 (d, 1H, *J* = 8.00 Hz, indole-H), 7.26 (s, 1H, Ph-H), 3.85 (s, 1H, piperidine-H), 3.41 (s, 2H, benzyl-CH_2), 3.17 (s, 3H, CH_3), 2.81 (d, 2H, *J* = 12.00 Hz, piperidine-H), 2.31 (s, 6H, 2×CH_3), 2.24 (t, 2H, *J* = 12.00 Hz, piperidine-H), 1.93 (d, 2H, *J* = 12.00 Hz, piperidine-H), 1.62 (q, 2H, *J* = 12.00 Hz, piperidine-H). ^{13}C NMR (100MHz, DMSO-d_6, ppm) δ: 159.04 (C=O), 155.89 (C=O), 145.35, 143.03, 139.43 (2×C), 137.84, 135.15, 133.28, 127.68, 125.70, 125.09, 124.12 (2×C), 119.35, 115.32, 111.73, 53.41 (CH_2), 51.79 (CH_2), 49.07 (CH_2), 47.05 (CH), 31.52 (2×CH_2), 27.28 (CH_3), 21.23 (2×CH_3). HRMS: m/z 557.1745 (M+1). $C_{26}H_{29}ClN_6O_4S$ [556.17].

*4.1.17. N-(1-(4-Sulfonamido-benzyl)piperidin-4-yl)-5-chloro-3-(3,5-dimethylphenyl-sulfonyl)-1H-indole-2-carboxamide (**19**)*

White solid, yield: 52.1%. mp: 215-217 °C. ^{1}H NMR (400MHz, DMSO-d_6, ppm) δ: 13.01 (s, 1H, Indole-NH), 8.97 (d, 1H, *J* = 8.00 Hz, CONH), 7.94 (s, 1H, indole-H), 7.81(d, 2H, *J* = 8.00 Hz, Ph'-H), 7.63 (s, 2H, Ph-H), 7.55-7.50 (m, 3H, indole-H, SO_2NH_2), 7.36-7.32 (m, 3H, Ph'-H, SO_2NH_2), 7.26(s, 1H, Ph-H), 3.87 (s, 1H, piperidine-H), 3.57 (s, 2H, benzyl-CH_2), 2.81 (d, 2H, *J* = 12.00 Hz, piperidine-H), 2.31 (s, 6H, 2×CH_3), 2.20 (t, 2H, *J* = 12.00 Hz, piperidine-H), 1.94 (d, 2H, *J* = 12.00 Hz, piperidine-H), 1.63 (q, 2H, *J* = 12.00 Hz, piperidine-H). ^{13}C NMR (100MHz, DMSO-d_6, ppm) δ: 159.01 (C=O), 143.20, 143.03, 139.44 (2×C), 137.84, 135.15,

133.29, 129.41 (2×C), 127.69, 126.11 (2×C), 125.72, 125.10, 124.11 (2×C), 119.35, 115.34, 111.72, 61.87 (CH_2), 52.10 (2×CH_2), 47.22 (CH), 31.65 (2×CH_2), 21.24 (2×CH_3). ESI-MS: m/z 615.3 (M+1). $C_{29}H_{31}ClN_4O_5S_2$ [614.14].

*4.1.18.N-(1-(4-Carbamoylbenzyl)piperidin-4-yl)-5-chloro-3-(3,5-dimethylphenyl-sulfonyl)-1H-indole-2-carboxamide (**20**)*

White solid, yield: 56.6%. mp: 153-155 °C. ^{1}H NMR (400MHz, DMSO-d_6, ppm) δ: 13.01 (s, 1H, indole-NH), 8.97 (d, 1H, *J* = 8.00 Hz, CONH), 7.94 (s, 2H, indole-H), 7.86 (d, 2H, *J* = 8.00 Hz, Ph'-H), 7.63 (s, 2H, Ph-H), 7.55-7.53 (d, 1H, indole-H), 7.40-7.32 (m, 4H, Ph'-H, $CONH_2$), 7.26 (s, 1H, Ph-H), 3.87 (s, 1H, piperidine-H), 3.54 (s, 2H, benzyl-CH_2), 2.81 (d, 2H, *J* = 12.00 Hz, piperidine-H), 2.31 (s, 6H, 2×CH_3), 2.18 (t, 2H, *J* = 12.00 Hz, piperidine-H), 1.94 (d, 2H, *J* = 12.00 Hz, piperidine-H), 1.63 (q, 2H, *J* = 12.00 Hz, piperidine-H). ^{13}C NMR (100MHz, DMSO-d_6, ppm) δ: 168.25 (C=O), 159.01 (C=O), 143.03, 139.43 (2×C), 137.87, 135.15, 133.46, 133.28, 128.87, 127.93 (4×C), 127.68, 125.70, 125.10, 124.12 (2×C), 119.35, 115.33, 111.72, 60.22 (CH_2), 52.09 (2×CH_2), 47.25 (CH), 31.64 (2×CH_2), 21.24 (2×CH_3). HRMS: m/z 579.1874 (M+1). $C_{30}H_{31}ClN_4O_4S$ [578.18].

*4.1.19. General procedure for the synthesis of target compounds (**21-25**)*

A solution of intermediate **6b** (0.10 g, 0.178 mmol, 1 equiv) in THF/MeOH (1/2, 30 mL) was treated with glacial acetic acid under stirring to adjust the pH value of 4-5. Then the aromatic aldehydes (RCHO) (0.535 mmol, 3 equiv) was added and the mixture was stirred for 40 minutes followed by addition of sodium cyanoborohydride (0.056 g, 0.89 mmol, 5 equiv). After additional 10 h, the solvent was evaporated under reduced pressure and the residues were dissovled with a small amount CH_2Cl_2 and chromatographed on silica gel using EA-PE system. Pure fractions were collected, concentrated and recrystallized, giving the desired compounds **21-25**.

*4.1.20.5-Chloro-3-(3,5-dimethylphenylsulfonyl)-N-(1-(thiophen-3-ylmethyl)-piperidin-4-yl)-1H-indole-2-carboxamide (**21**)*

White solid, yield: 70.2%. mp: 230-231 °C. ^{1}H NMR (400MHz, DMSO-d_6, ppm)δ: 12.92 (s, 1H, indole-NH), 8.99 (d, 1H, *J* = 8.00 Hz, CONH), 7.94 (s, 1H,

indole-H), 7.63-7.54 (m, 4H, thiophene-H,Ph-H), 7.44(d, 1H, *J* = 8.00 Hz, indole-H), 7.24(d, 1H, *J* = 8.00 Hz, indole-H), 7.15-7.13 (m, 2H, thiophene-H,Ph-H), 4.21 (s, 2H, thiophene-CH_2), 3.99 (s, 1H, piperidine-H), 3.34 (s, 2H, piperidine-H), 3.00 (s, 2H, piperidine-H), 2.20 (s, 6H, 2×CH_3), 2.04 (s, 2H, piperidine-H), 1.64 (s, 2H, piperidine-H). ESI-MS: m/z 542.4 (M+1). $C_{27}H_{28}ClN_3O_3S_2$ [541.13].

*4.1.21.5-Chloro-3-(3,5-dimethylphenylsulfonyl)-N-(1-(thiophen-3-ylmethyl) piperidin-4-yl)-1H-indole-2-carboxamide (**22**)*

White solid, yield: 69.6%. mp: 225-256 °C. ESI-MS: m/z 542.4 (M+1). $C_{27}H_{28}ClN_3O_3S_2$ [541.13].

*4.1.22.N-(1-(4-(Trifluoromethyl)benzyl)piperidin-4-yl)-5-chloro-3-(3,5-dimethylphen-ylsulfonyl)-1H-indole-2-carboxamide (**23**)*

White solid, yield: 69.8%. mp: 209-210 °C. ^{1}H NMR (400MHz, DMSO-d_6, ppm) δ: 13.00 (s, 1H, indole-NH), 8.97 (d, 1H, *J* = 8.00 Hz, CONH), 7.95 (s, 1H, indole-H), 7.70(d, 2H, *J* = 8.00 Hz, Ph'-H), 7.63(s, 2H, Ph-H), 7.56-7.53(m, 3H, *J* = 8.00 Hz, indole-H, Ph'-H), 7.35(d, 1H, *J* = 8.00 Hz, indole-H), 7.26(s, 1H, Ph-H), 3.88 (s, 1H, piperidine-H), 3.59 (s, 2H, benzyl-CH_2), 2.81 (d, 2H, *J* = 12.00 Hz, piperidine-H), 2.31 (s, 6H, 2×CH_3), 2.21 (t, 2H, *J* = 12.00 Hz, piperidine-H), 1.94 (d, 2H, *J* = 12.00 Hz, piperidine-H), 1.64 (q, 2H, *J* = 12.00 Hz, piperidine-H). ^{13}C NMR (100MHz, DMSO-d_6, ppm) δ: 159.02 (C=O), 144.21, 143.05, 139.43 (2×C), 137.87, 135.14, 133.31, 129.71 (2×C), 128.18, 127.87, 127.68, 126.61, 125.73, 125.47, 125.08, 124.11 (2×C), 119.35, 115.34, 111.72, 61.83 (CH_2), 52.08 (2×CH_2), 47.21 (CH), 31.66 (2×CH_2), 21.23 (2×CH_3). ESI-MS: m/z 604.4 (M+1). $C_{30}H_{29}ClF_3N_3O_3S$ [603.16].

*4.1.23.5-Chloro-3-(3,5-dimethylphenylsulfonyl)-N-(1-(furan-3-ylmethyl)piperidin-4-yl)-1H-indole-2-carboxamide (**24**)*

White solid, yield: 68.8%. mp: 223-224 °C. ^{1}H NMR (400MHz, DMSO-d_6, ppm) δ: 12.91 (s, 1H, indole-NH), 8.98 (d, 1H, *J* = 8.00 Hz, CONH), 7.79 (s, 1H, indole-H), 7.72 (s, 1H, furan-H), 7.53 (s, 2H, Ph-H), 7.44 (d, 1H, *J* = 8.00 Hz, indole-H), 7.24 (d, 1H, *J* = 8.00 Hz, indole-H), 7.14 (s, 1H, Ph-H), 6.57 (s, 1H, furan-H), 6.46 (s, 1H, furan-H), 4.24 (s, 2H, thiophene-CH_2), 3.98 (s, 1H, piperidine-H), 3.31 (s, 2H, piperidine-H), 2.98 (s, 2H, piperidine-H), 2.20 (s, 6H, 2×CH_3), 2.00 (s, 2H,

piperidine-H), 1.65 (s, 2H, piperidine-H). HRMS: m/z 526.1573 (M+1). $C_{27}H_{28}ClN_3O_4S$ [525.15].

*4.1.24.N-(1-(4-Nitrobenzyl)piperidin-4-yl)-5-chloro-3-(3,5-dimethylphenylsulfonyl)-1H-indole-2-carboxamide (**25**)*

White solid, yield: 65.6%. mp: 258-259 °C, decomposition. ^{1}H NMR (400MHz, DMSO-d_6, ppm) δ: 13.01 (s, 1H, indole-NH), 8.97 (d, 1H, *J* = 8.00 Hz, CONH), 8.21 (d, 2H, *J* = 8.00 Hz, Ph'-H), 7.94 (s, 1H, indole-H), 7.63-7.60 (m, 4H, Ph-H, Ph'-H), 7.55 (d, 1H, *J* = 8.00 Hz, indole-H), 7.35 (d, 1H, *J* = 8.00 Hz, indole-H), 7.26 (s, 1H, Ph-H), 3.88 (s, 1H, piperidine-H), 3.63 (s, 2H, benzyl-CH_2), 2.81 (d, 2H, *J* = 8.00 Hz, piperidine-H), 2.31 (s, 6H, 2×CH_3), 2.23 (t, 2H, *J* = 8.00 Hz, piperidine-H), 1.95 (d, 2H, *J* = 12.00 Hz, piperidine-H), 1.64 (q, 2H, *J* = 8.00 Hz, piperidine-H). ^{13}C NMR (100MHz, DMSO-d_6, ppm) δ: 159.01(C=O), 147.59, 147.01, 143.03, 139.43 (2×C), 137.84, 135.15, 133.29, 130.02 (2×C), 127.68, 125.71, 125.10, 124.11 (2×C), 123.85 (2×C), 119.35, 115.53, 111.72, 61.55 (CH_2), 52.08 (2×CH_2), 47.14 (CH), 31.65 (2×CH_2), 21.24(2×CH_3). ESI-MS: m/z 581.4 (M+1). $C_{29}H_{29}ClN_4O_5S$ [580.15].

*4.1.25.5-Chloro-3-(3,5-dimethylphenylsulfonyl)-N-((1-(2-hydroxyethyl)piperidin-4-yl) methyl)-1H-indole-2-carboxamide (**26**)*

White solid, yield: 50.0%. mp: 255-256 °C. ^{1}H NMR (400MHz, DMSO-d_6, ppm) δ: 13.02 (s, 1H, indole-NH), 9.08 (d, 1H, *J* = 4.00 Hz, CONH), 7.88 (s, 1H, indole-H), 7.65 (s, 2H, Ph-H), 7.55 (s, 1H, *J* = 8.00 Hz, indole-H), 7.35 (s, 1H, *J* = 8.00 Hz, indole-H), 7.27 (s, 1H, Ph-H), 5.28 (s, 1H, OH), 3.37 (s, 2H, CH_2), 3.50 (s, 2H, CH_2), 3.40 (s, 2H, CH_2), 3.11 (s, 2H, CH_2), 2.31 (s, 6H, 2×CH_3), 2.29 (s, 2H, CH_2), 1.98 (s, 2H, CH_2), 1.86 (s, 1H, CH), 1.53 (s, 2H, CH_2). HRMS: m/z 504.1772 (M+1). $C_{25}H_{30}ClN_3O_4S$ [503.16].

*4.1.26.N-((1-(4-Carbamoylbenzyl)piperidin-4-yl)methyl)-5-chloro-3-(3,5-dimethyl-phenylsulfonyl)-1H-indole-2-carboxamide (**27**)*

White solid, yield: 52.3%. mp: 259-260 °C. ^{1}H NMR (400MHz, DMSO-d_6, ppm) δ: 12.93 (s, 1H, indole-NH), 8.98 (d, 1H, *J* = 8.00 Hz, CONH), 7.92-7.90 (m, 2H, indole-H, NH_2), 7.83 (d, 2H, *J* = 8.00 Hz, Ph'-H), 7.61 (s, 2H, Ph-H), 7.54 (d, 1H, *J* = 8.00 Hz, indole-H), 7.37-7.52 (m, 5H, indole-H, NH_2, Ph-H, Ph'-H), 3.50 (s, 2H,

benzyl-CH_2), 3.32-3.24 (m, 2H, CONH-CH_2), 2.83 (d, 2H, *J* = 12.00 Hz, piperidine-H), 2.30 (s, 6H, 2×CH_3), 1.98 (t, 2H, *J* = 8.00 Hz, piperidine-H), 1.76 (d, 2H, *J* = 8.00 Hz, piperidine-H), 1.57 (s, 1H, piperidine-H), 1.62 (q, 2H, *J* = 8.00 Hz, piperidine-H). ^{13}C-NMR (100MHz, DMSO-d_6, ppm) δ: 168.26 (C=O), 159.86 (C=O), 143.07, 142.49, 139.40 (2×C), 137.95, 135.12, 133.38, 133.34, 128.89 (2×C), 127.86 (2×C), 127.64, 125.77, 125.05, 124.09 (2×C), 119.33, 115.36, 111.53, 62.38 (CH_2), 53.40 (2×CH_2), 45.40 (CH), 36.07 (CH_2), 30.09 (2×CH_2), 21.24 (2×CH_3). ESI-MS: m/z 593.5 (M+1). $C_{31}H_{33}ClN_4O_4S$ [592.19].

*4.1.27.N-((1-(3-Fluorobenzyl)piperidin-4-yl)methyl)-5-chloro-3-(3,5-dimethylphenyl -sulfonyl)-1H-indole-2-carboxamide (**28**)*

White solid, yield: 46.5%. mp: 193-194 °C. ^{1}H NMR (400MHz, DMSO-d_6, ppm) δ:13.00 (s, 1H, indole-NH), 8.97 (d, 1H, *J* = 8.00 Hz, CONH), 7.92 (d, 1H, *J* = 12.00 Hz, indole-H), 7.61 (s, 2H, Ph-H), 7.54 (d, 1H, *J* = 8.00 Hz, indole-H), 7.37-7.31 (m, 2H, indole-H, Ph'-H), 7.26 (s, 1H, Ph-H), 7.14-7.04 (m, 3H, Ph'-H), 3.47 (s, 2H, benzyl-CH_2), 3.27 (t, 2H, *J* = 8.00 Hz, CONH-CH_2), 2.82 (d, 2H, *J* = 12.00 Hz, piperidine-H), 2.30 (s, 6H, 2×CH_3), 1.97 (t, 2H, *J* = 12.00 Hz, piperidine-H), 1.94 (d, 2H, *J* = 2.00 Hz, piperidine-H), 1.57 (s, 1H, piperidine-H), 1.30 (q, 2H, *J* = 12.00 Hz, piperidine-H). ^{13}C-NMR (100MHz, DMSO-d_6, ppm) δ: 161.26 (C-F), 159.86 (C=O), 143.10, 139.38 (2×C), 137.98, 135.09, 133.40, 130.50, 130.42, 127.61, 125.81, 125.10, 124.10 (2×C), 119.33, 115.63, 115.39, 114.14, 113.93, 111.53, 62.05 (CH_2), 53.40 (2×CH_2), 45.37 (CH), 36.06 (CH_2), 30.08 (2×CH_2), 21.23 (2×CH_3). ESI-MS: m/z 568.5 (M+1). $C_{30}H_{31}ClFN_3O_3S$ [567.18].

*4.1.28.N-((1-(3-Cyanobenzyl)piperidin-4-yl)methyl)-5-chloro-3-(3,5-dimethylphenyl -sulfonyl)-1H-indole-2-carboxamide (**29**)*

White solid, yield: 52.6%. mp: 213-214 °C. ^{1}H NMR (400MHz, DMSO-d_6, ppm) δ:13.00 (s, 1H, indole-NH), 8.96 (d, 1H, *J* = 8.00 Hz, CONH), 7.92 (s, 1H, indole-H), 7.80 (d, 1H, *J* = 4.00 Hz, Ph'-H), 7.68 (t, 1H, *J* = 8.00 Hz, Ph'-H), 7.61 (s, 2H, Ph-H), 7.57-7.30 (m, 4H, indole-H, Ph'-H), 7.24 (s, 1H, Ph-H), 3.63 (s, 2H, benzyl-CH_2), 3.26 (t, 2H, *J* = 8.00 Hz, CONH-CH_2), 2.82 (d, 2H, *J* = 12.00 Hz, piperidine-H), 2.30 (s, 6H, 2×CH_3), 2.06 (t, 2H, *J* = 12.00 Hz, piperidine-H), 1.76 (d, 2H, *J* = 12.00 Hz,

piperidine-H), 1.59 (s, 1H, piperidine-H), 1.29 (q, 2H, *J* = 12.00 Hz, piperidine-H). ^{13}C-NMR (100MHz, DMSO-d_6, ppm) δ: 159.86 (C=O), 143.10, 142.95, 139.35 (2×C), 138.11, 138.06, 135.06, 133.50, 133.41, 130.51, 128.35, 127.56, 125.86, 124.95, 124.12 (2×C), 119.32, 118.19, 115.43, 112.51, 111.51, 60.56 (CH_2), 53.36 (2×CH_2), 45.33 (CH), 35.97 (CH_2), 30.06 (2×CH_2), 21.24 (2×CH_3). ESI-MS: m/z 575.5(M+1). $C_{31}H_{31}ClN_4O_3S$ [574.18].

*4.1.29.Ethyl3-(4-((5-chloro-3-(3,5-dimethylphenylsulfonyl)-1H-indole-2-carboxamido)methyl)piperidin-1-yl)propanoate (**30**)*

White solid, yield: 45.6%. mp: 194-195 °C. ^{1}H NMR (400MHz, DMSO-d_6, ppm) δ:13.01 (s, 1H, indole-NH), 8.96 (s, 1H,CONH), 7.92 (s, 1H,indole-H), 7.61 (s, 2H, Ph-H), 7.80 (d, 1H, *J* = 8.00 Hz, indole-H), 7.34 (d, 1H, *J* = 8.00 Hz, indole-H), 7.26 (s, 1H, Ph-H), 4.07 (q, 2H, *J* = 4.00 Hz, O-CH_2), 3.25 (t, 2H, *J* = 4.00 Hz, CO-CH_2), 2.82 (d, 2H, *J* = 12.00 Hz, piperidine-H), 2.57 (d, 2H, *J* = 8.00 Hz, CH_2), 2.46 (d, 2H, *J* = 8.00 Hz, CH_2), 2.31 (s, 6H, 2×CH_3), 1.98 (t, 2H, *J* = 12.00 Hz, piperidine-H), 1.75 (d, 2H, *J* = 12.00 Hz, piperidine-H), 1.56 (s, 1H, piperidine-H), 1.25-1.15 (m, 5H, piperidine-H, CH_3). ^{13}C-NMR (100MHz, DMSO-d_6, ppm) δ: 172.46 (C=O), 159.85 (C=O), 143.06, 139.41 (2×C), 137.94, 135.12, 133.34, 127.63, 125.75, 125.05, 124.10 (2×C), 119.32, 115.35, 111.51, 60.19 (CH_2), 53.92 (2×CH_2), 53.20, 45.38 (CH), 36.02 (CH_2), 32.37, 30.03 (2×CH_2), 21.24 (2×CH_3), 14.59. ESI-MS: m/z 560.4(M+1). $C_{28}H_{34}ClN_3O_5S$ [559.19].

4.2. *In vitro* anti-HIV assay

Evaluation of the antiviral activity and cytotoxicity of the compounds in MT-4 cells was performed using the MTT assay as previously described [33,52]. Stock solutions (10×final concentration) of test compounds were added in 25 µL volumes to two series of triplicate wells so as to allow simultaneous evaluation of their effects on mock- and HIV-infected cells at the beginning of each experiment. Serial five-fold dilutions of test compounds were made directly in flat-bottomed 96wells microtiter trays using a Biomek 3000 robot (Beckman instruments, Fuller-ton, CA). Untreated control HIV- and mock-infected cell samples were included for each sample.

HIV-1(IIIB), single and double RT mutant strains (L100I, K103N, Y181C, Y188L, E138K, F227L/V106A, RES056) or HIV-2 (ROD) [53] stock (50µL) at 100-300 CCID50 (cell culture infectious dose) or culture medium was added to either the infected or mock-infected wells of the microtiter tray. Mock-infected cells were used to evaluate the effect of test compounds on uninfected cells in order to assess the cytotoxicity of the test compound. Exponentially growing MT-4 cells were cen-trifuged for 5 minutes at 1000 rpm and the supernatant was discarded. The MT-4 cells were resuspended at 6×10^5 cells/mL, and 50-µL volumes were transferred to the microtiter tray wells. Five days after infection, the viability of mock- and HIV-infected cells was examined spectrophotometrically by the MTT assay. The 50% cytotoxic concentration (CC_{50}) was defined as the concentration of the test compound that reduced the absorbance (OD540) of the mock-in-fected control sample by 50%. The concentration achieving 50% protection from the cytopathic effect of the virus in infected cells was defined as the 50% effective concentration (EC_{50}).

4.3. HIV-1 RT inhibition assay

A reverse transcriptase (RT) assay kit produced by Roche was selected for the RT inhibition assay. All the reagents for performing the RT reaction came with the kit and the ELSIA procedures for RT inhibition assay was carried out following the description in the kit protocol [54,55]. Briefly, the reaction mixture containing template/primer complex, viral nucleotides (dNTPs) and RT in the incubation buffer with or without inhibitors was incubated for 1hours at 37 °C. After that, the reaction mixture was transferred to a streptavidine-coated microtiter plate and incubated for another 1hours at 37 °C to make sure retranscriptional cDNA chain that consisted biotin-labeled dNTPs bound to streptavidine. Then removed un-bound dNTPs using washing buffer and added anti-DIG-POD working solution. After incubation for 1hours at 37 °C, the DIG-labeled dNTPs incorporated in cDNA were bound to the anti-DIG-POD antibody. The unbound anti-DIG-PODs were removed and the peroxidesubstrate (ABST) solution was added to the MTPs. A colored reaction proceed during cleavage of the substrate catalyzed by POD. The absorbance of the

sample was determined at OD 405 nm using a microtiter plate ELISA reader. The percentage inhibitory activity of RT inhibitors was calculated byformula as given below:

%Inhibition = [OD value with RT but without inhibitors - OD value with RT and inhibitors]/[OD value with RT and inhibitors - OD value without RT and inhibitors]

The IC_{50} values corresponded to the concentrations of the in-hibitors required to inhibit biotin-dUTP incorporation by 50%.

4.4. Molecular simulation experiment

The molecules **8** and **18** for docking was optimized for 2000-generations until the maximum derivative of energy became 0.005 kcal/(mol*A), using the Tripos force field. Charges were computed and added according to Gasteiger-Huckel parameters. The published three dimensional crystal structures of RT complexes (PDB code: 2rf2) were retrieved from the Protein Data Bank and were used for the docking experiment by means of surflex-docking module of Sybyl-X 1.1. The protein was prepared by using the Biopolymer application accompanying Sybyl: The bound ligand was extracted from the complexes, water molecules were removed, hydrogen atoms were added, side chain amides and side chains bumps were fixed, and charges and atom types were assigned according to AMBER 99. After the protomol was generated, the optimized **8** and **18** were surflex-docked into the binding pocket of NNRTIs, with the relevant parameters set as defaults. Top-scoring pose was shown by the software of PyMOL version 1.5 (www.pymol.org.). The secondary structure of RT is shown in cartoons, and only the key residues for interactions with the inhibitor were shown in sticks and labeled. The potential hydrogen bonds were presented by dashed lines.

Conflict of interest

The authors declare no conflict of interest.

Acknowledgments

We thank K. Erven, K. Uyttersprot and C. Heens for technical assistance with the HIV assays. The financial support from the National Natural Science Foundation of China (NSFC Nos. 81273354, 81573347), Key Project of NSFC for International

Cooperation (No. 81420108027), The Natural Science Foundation of Shandong Province (No. ZR2009CM016), Young Scholars Program of Shandong University (YSPSDU, No. 2016WLJH32, to P.Z.), Major Project of Science and Technology of Shandong Province (No. 2015ZDJS04001) and KU Leuven (GOA 10/014).

References

[1] LO. Kallings, The first postmodern pandemic: 25 years of HIV/AIDS, J. Intern. Med. 263 (2008) 218-243.

[2] Global Report: UNAIDS report on the global AIDS epidemic (2015).

[3] E. De Clercq, Anti-HIV drugs: 25 compounds approved within 25 years after the discovery of HIV, Int. J. Antimicrob Agents 33 (2009) 307-320.

[4] Y. Mehellou, E. De Clercq, Twenty-six years of anti-HIV drug discovery: where do we stand and where do we go? J. Med. Chem. 53(2010) 521-538.

[5] D.M. Margolis, D.J. Hazuda, Combined approaches for HIV cure, Curr. Opin. HIV AIDS. 8 (2013) 230-235.

[6] M.P. de Béthune, Non-nucleoside reverse transcriptase inhibitors (NNRTIs), their discovery, development, and use in the treatment of HIV-1 infection: a review of the last 20 years (1989-2009), Antiviral Res. 85 (2010) 75-90.

[7] S. Martins, M.J. Ramos, P.A. Fernandes, The current status of the NNRTI family of antiretrovirals used in the HAART regime against HIV infection, Curr. Med. Chem. 15 (2008) 1083-1095.

[8] P. Zhan, X. Chen, D. Li, Z. Fang, E. De Clercq, X. Liu, HIV-1 NNRTIs: structural diversity, pharmacophore similarity, and impliations for drug design, Med. Res. Rev. 33 (2013) E1-E72.

[9] P. Zhan, X. Liu, Novel HIV-1 non-nucleoside reverse transcriptase inhibitors: a patent review (2005 - 2010), Expert Opin. Ther. Pat. 21 (2011) 717-796.

[10] X. Li, L. Zhang, Y. Tian, Y. Song, P. Zhan, X. Liu, Novel HIV-1 non-nucleoside reverse transcriptase inhibitors:a patent review (2011-2014), Expert Opin, Ther, Pat. 24 (2014) 1199-1227.

[11] P. Zhan, X. Liu, Z. Li, Recent advances in the discovery and development of novel HIV-1 NNRTI platforms: 2006-2008 update, Curr. Med. Chem. 16 (2009) 2876–2889.

[12] Y. Song, Z. Fang, P. Zhan, X. Liu, Recent Advances in the Discovery and Development of Novel HIV-1 NNRTI Platforms (Part II): 2009-2013 Update, Curr. Med. Chem. 21 (2014)

329-355.

[13] J. Guillemont, E. Pasquier, P. Palandjian, D. Vernier, S. Gaurrand, P.J. Lewi, J. Heeres, M.R. de Jonge, L.M. Koymans, F.F. Daeyaert, M.H. Vinkers, E. Arnold, K. Das, R. Pauwels, K. Andries, M.P. de Béthune, E. Bettens, K. Hertogs, P. Wigerinck, P. Timmerman, P.A. Janssen, Synthesis of novel diarylpyrimidine analogues and their antiviral activity against human immunodeficiency virus type 1, J. Med. Chem. 48 (2005) 2072-2079.

[14] X. Chen, P. Zhan, D Li, E. De Clercq, X. Liu, Recent advances in DAPYs and related analogues as HIV-1 NNRTIs, Curr. Med. Chem. 18 (2011) 359–376.

[15] R. Schrijvers, Etravirine for the treatment of HIV/AIDS, Expert Opin. Pharmaco. Ther. 14 (2013) 1087-1096.

[16] J.J. Minudo, R. Haubrich, Entravirine: a second-generation NNRTI for treatment-experienced adults with resistant HIV-1 infection, Futur. HIV Ther. 2 (2008) 525–537.

[17] L. Rimsky, J. Vingerhoets, V. Van Eygen, J. Eron, B. Clotet, A. Hoogstoel, K. Boven, G. Picchio, Genotypic and phenotypic characterization of HIV-1 isolates obtained from patients on rilpivirine therapy experiencing virologic failure in the phase 3 ECHO and THRIVE studies: 48-week analysis, J. Acquir. Immune. Defic. Syndr. 59 (2012) 39–46.

[18] P. Zhan, C. Pannecouque, E. De Clercq, X. Liu, Anti-HIV drug discovery and development: Current innovations and future trends, J. Med. Chem. 59 (2016) 2849–2878.

[19] D. Li, P. Zhan, E. De Clercq, X. Liu, Strategies for the design of HIV-1 nonnucleoside reverse transcriptase inhibitors: lessons from the development of seven representative paradigms, J. Med. Chem. 55 (2012) 3595–3613.

[20] T.M. Williams, T.M. Ciccarone, S.C. MacTough, C.S. Rooney, S.K. Balani, J.H. Condra, E.A. Emini, M.E. Goldman, W.J. Greenlee, L.R. Kauffman, 5-chloro-3-(phenylsulfonyl)indole-2-carboxamide: a novel, non-nucleoside inhibitor of HIV-1 reverse transcriptase, J. Med. Chem. 36 (1993) 1291-1294.

[21] R. Silvestri, G. De Martino, G. La Regina, M. Artico, S. Massa, L. Vargiu, M. Mura, A.G. Loi, T. Marceddu, P. La Colla, Novel indolyl aryl sulfones active against HIV-1 carrying NNRTI resistance mutations: synthesis and SAR studies, J. Med. Chem. 46 (2003) 2482-2493.

[22] R. Silvestri, M. Artico, G. De Martino, G. La Regina, R. Loddo, M. La Colla, M. Mura, P. La Colla, Simple, short peptide derivatives of a sulfonylindolecarboxamide (L-737,126) active in

vitro against HIV-1 wild type and variants carrying non-nucleoside reverse transcriptase inhibitor resistance mutations. J. Med. Chem. 47 (2004) 3892-3896.

[23] G. La Regina, A. Coluccia, A. Brancale, F. Piscitelli, V. Famiglini, S. Cosconati, G. Maga, A. Samuele, E. Gonzalez, B. Clotet, D. Schols, J.A .Esté, E. Novellino, R. Silvestri, New nitrogen containing substituents at the indole-2-carboxamide yield high potent and broad spectrum indolylarylsulfone HIV-1 non-nucleoside reverse transcriptase inhibitors, J. Med. Chem. 55 (2012) 6634-6638. .

[24] G. La Regina, A. Coluccia, A. Brancale, F. Piscitelli, V. Gatti, G. Maga, A. Samuele, C. Pannecouque, D. Schols, J. Balzarini, E. Novellino, R. Silvestri, Indolylarylsulfones as HIV-1 non-nucleoside reverse transcriptase inhibitors: new cyclic substituents at indole-2-carboxamide, J. Med. Chem. 54 (2011) 1587-1598.

[25] R. Ragno, A. Coluccia, G. La Regina, G. De Martino, F. Piscitelli, A. Lavecchia, E. Novellino, A. Bergamini, C. Ciaprini, A. Sinistro, G. Maga, E. Crespan, M. Artico, R. Silvestri, Design, molecular modeling, synthesis, and anti-HIV-1 activity of new indolyl aryl sulfones. Novel derivatives of the indole-2-carboxamide, J. Med. Chem. 49 (2006) 3172-3184.

[26] F. Piscitelli, A. Coluccia, A. Brancale, G. La Regina, A. Sansone, C. Giordano, J. Balzarini, G. Maga, S. Zanoli, A. Samuele, R. Cirilli, F. La Torre, A. Lavecchia, E. Novellino, R. Silvestri, Indolylarylsulfones bearing natural and unnatural amino acids. Discovery of potent inhibitors of HIV-1 non-nucleoside wild type and resistant mutant strains reverse transcriptase and coxsackie B4 virus, J. Med. Chem. 52 (2009) 1922-1934.

[27] Z. Zhao, S.E. Wolkenberg, P.E. Sanderson, M. Lu, V. Munshi, G. Moyer, M. Feng, A.V. Carella, L.T. Ecto, L.J. Gabryelski, M.T. Lai, S.G. Prasad, Y. Yan, G.B. McGaughey, M.D. Miller, C.W. Lindsley, G.D. Hartman, J.P. Vacca, T.M. Williams, Novel indole-3-sulfonamides as potent HIV non-nucleoside reverse transcriptase inhibitors (NNRTIs), Bioorg. Med. Chem. Lett. 18 (2008) 554-559.

[28] M.Z. Zhang, Q. Chen, G.F. Yang, A review on recent developments of indole-containing antiviral agents, Eur J Med Chem. 89 (2015) 421-441.

[29] G.F. Hao, G.F. Yang, C.G. Zhan, Computational mutation scanning and drug resistance mechanisms of HIV-1 protease inhibitors, J PhysChem B. 114 (2010) 9663-9676.[30] G. Tang, D.J. Kertesz, M. Yang, X. Lin, Z. Wang, W. Li, Z. Qiu, J. Chen, J. Mei, L. Chen, T. Mirzadegan, S.F.

Harris, A.G. Villaseñor, J. Fretland, W.L. Fitch, J.Q. Hang, G. Heilek, K. Klumpp, Exploration of piperidine-4-yl-aminopyrimidines as HIV-1 reverse transcriptase inhibitors. N-Phenyl derivatives with broad potency against resistant mutant viruses, Bioorg. Med. Chem. Lett. 2 (2010) 6020-6023.

[31] D.J. Kertesz, C. Brotherton-Pleiss, M. Yang, Z. Wang, X. Lin, Z. Qiu, D.R. Hirschfeld, S. Gleason, T. Mirzadegan, P.W. Dunten, S.F. Harris, A.G. Villaseñor, J.Q. Hang, G.M. Heilek, K. Klumpp, Discovery of piperidin-4-yl-aminopyrimidines as HIV-1 reverse transcriptase inhibitors. N-benzyl derivatives with broad potency against resistant mutant viruses, Bioorg. Med. Chem. Lett. 20 (2010) 4215-4218

[32] B. Huang, C. Li, W. Chen, T. Liu, M. Yu, L. Fu, Y. Sun, H. Liu, E. De Clercq, C. Pannecouque, J. Balzarini, P. Zhan, X. Liu, Fused heterocycles bearing bridgehead nitrogen as potent HIV-1 NNRTIs. Part 3: optimization of [1,2,4]triazolo[1,5-a]pyrimidine core via structure-based and physicochemical property-driven approaches, Eur. J. Med. Chem. 92 (2015) 754-765.

[33] X. Chen, Y. Li, S. Ding, J. Balzarini, C. Pannecouque, E. De Clercq, H. Liu, X. Liu, Discovery of piperidine-linked pyridine analogues as potent non-nucleoside HIV-1 reverse transcriptase inhibitors, ChemMedChem. 8 (2013) 1117-1126.

[34] X. Chen, X. Liu, Q. Meng, D. Wang, H. Liu, E. De Clercq, C. Pannecouque, J. Balzarini, X. Liu, Novel piperidinylamino-diarylpyrimidine derivatives with dual structural conformations as potent HIV-1 non-nucleoside reverse transcriptase inhibitors, Bioorg. Med. Chem. Lett. 23 (2013) 6593-6597.

[35] X. Chen, P. Zhan, C. Pannecouque, J. Balzarini, E. De Clercq, X. Liu, Synthesis and biological evaluation of piperidine-substituted triazine derivatives as HIV-1 non-nucleoside reverse transcriptase inhibitors, Eur. J. Med. Chem. 51 (2012) 60-66.

[36] X. Chen, P. Zhan, X. Liu, Z. Cheng, C. Meng, S. Shao, C. Pannecouque, E. De Clercq, X. Liu, Design, synthesis, anti-HIV evaluation and molecular modeling of piperidine-linked amino-triazine derivatives as potent non-nucleoside reverse transcriptase inhibitors, Bioorg. Med. Chem. 20 (2012) 3856-3864.

[37] L. Zhang, P. Zhan, X. Chen, Z. Li, Z. Xie, T. Zhao, H. Liu, E. De Clercq, C. Pannecouque, J. Balzarini, X. Liu, Design, synthesis and preliminary SAR studies of novel N-arylmethyl

substituted piperidine-linked aniline derivatives as potent HIV-1 NNRTIs, Bioorg. Med. Chem. 22 (2014) 633-642.

[38] Q. Meng, X. Chen, D. Kang, B. Huang, W. Li, P. Zhan, D. Daelemans, E. De Clercq, C. Pannecouque, X. Liu, Design, synthesis and evaluation of novel HIV-1 NNRTIs with dual structural conformations targeting the entrance channel of the NNRTI binding pocket, Eur. J. Med. Chem. 115 (2016) 53–62.

[39] J. Yang, W. Chen, D. Kang, X. Lu, X. Li, Z. Liu, B. Huang, D. Daelemans, C. Pannecouque, E. De Clercq, P. Zhan, X. Liu, Design, synthesis and anti-HIV evaluation of novel diarylpyridine derivatives targeting the entrance channel of NNRTI binding pocket, Eur. J. Med. Chem. 109 (2016) 294–304.

[40] X. Chen, Q. Meng, L. Qiu, P. Zhan, H. Liu, E. De Clercq, C. Pannecouque, X. Liu, Design, Synthesis, and Anti-HIV Evaluation of Novel Triazine Derivatives Targeting the Entrance Channel of the NNRTI Binding Pocket, Chem. Biol. Drug Des. 86 (2015) 122–128.

[41] Z. Liu, W. Chen, P. Zhan, E. De Clercq, C. Pannecouque, X. Liu, Design, synthesis and anti-HIV evaluation of novel diarylnicotinamide derivatives (DANAs) targeting the entrance channel of the NNRTI binding pocket through structure-guided molecular hybridization, Eur. J. Med. Chem. 87 (2014) 52–62.

[42] W. Chen, P. Zhan, D. Daelemans, J. Yang, B. Huang, E. De Clercq, C. Pannecouque, X. Liu, Structural optimization of pyridine-type DAPY derivatives to exploit the tolerant regions of the NNRTI binding pocket, Eur. J. Med. Chem. 121 (2016) 352–363.

[43] W. Chen, P. Zhan, D. Rai, E. De Clercq, C. Pannecouque, J. Balzarini, Z. Zhou, H. Liu, X. Liu, Discovery of 2-pyridone derivatives as potent HIV-1 NNRTIs using molecular hybridization based on crystallographic overlays. Bioorg Med Chem. 22 (2014) 1863-1872.

[44] W. Chen, P. Zhan, J. Wu, Z. Li, X. Liu, The development of HEPT-type HIV non-nucleoside reverse transcriptase inhibitors and its implications for DABO family, Curr Pharm Des. 18 (2012) 4165-4186.

[45] P. Zhan, X. Liu, Z. Li, C. Pannecouque, E. De Clercq, Design strategies of novel NNRTIs to overcome drug resistance, Curr. Med. Chem. 16 (2009) 3903–3917.

[46] Y. Song, P. Zhan, X. Li, D. Rai, E. De Clercq, X. Liu, Multivalent agents: a novel concept and preliminary practice in Anti-HIV drug discovery. Curr. Med. Chem. 20 (2013) 815–832.

[47] J.S. Yadav, B.V. Subba Reddy, Y. Jayasudhan Reddy, A rapid synthesis of 3-sulfenyl indoles using Selectfluor, Tetrahedron Lett. 48 (2007) 7034-7037.

[48] D. Zampieri, E. Laurini, L. Vio, M. Fermeglia, S. Pricl, B. Wünsch, D. Schepmann, M.G. Mamolo, Improving selectivity preserving affinity: new piperidine-4-carboxamide derivatives as effective sigma-1-ligands, Eur. J. Med. Chem. 90 (2015) 797-808.

[49] M.T. Barho, S. Oppermann, F.C. Schrader, I. Degenhardt, K. Elsässer, C. Wegscheid-Gerlach, C. Culmsee, M. Schlitzer, N-acyl derivatives of 4-phenoxyaniline as neuroprotective agents, ChemMedChem 9 (2014) 2260-2273.

[50] S.S. Carroll, D.B. Olsen, C.D. Bennett, L. Gotlib, D.J. Graham, J.H. Condra, A.M. Stern, J.A. Shafer, L.C. Kuo, Inhibition of HIV-1 reverse transcriptase by pyridinone derivatives. Potency, binding characteristics, and effect of template sequence, J. Biol. Chem. 268 (1993) 276–281.

[51] URL: http://www.certara.com/products/molmod/surflex/surflex-dock/.

[52] C. Pannecouque, D. Daelemans, E. De Clercq, Tetrazolium-based colorimetric assay for the detection of HIV replication inhibitors: revisited 20 years later, Nat. Protoc. 3 (2008) 427-434.

[53] F. Clavel, D. Guétard, F. Brun-Vézinet, S. Chamaret, M. A. Rey, M. O. Santos-Ferreira, A. G. Laurent, C. Dauguet, C. Katlama and Rouzioux, C.Isolation of a new human retrovirus from West African patients with AIDS, Science 233 (1986) 343-346.

[54] Reverse Transcriptase Assay, Colorimetric kit, Roche Diagnostics GmbH, Roche. Applied Science, SandhoferStrasse 116, D-68305 Mannheim, Germany.

[55] K. Suzuki, B.P. Craddock, N. Okamoto, T. Kano, R.T. Steigbigel, Poly A-linked colorimetric microtiter plate assay for HIV reverse transcriptase, J. Virol. Methods 44 (1993) 189-198.

Table 1. Activity against HIV-1 strains, cytotoxicity and selectivity indexin MT-4 cells.

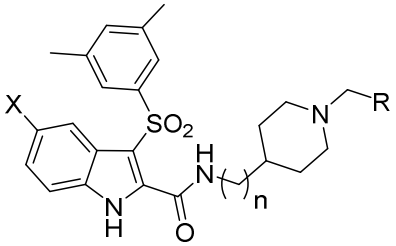

7-14: X = Br, n = 0;
15-25: X = Cl, n = 0;
26-30: X = Cl, n = 1

com	R	EC_{50} (μM)[a]								CC_{50}
pd		IIIB	L100I	K103N	Y181C	Y188L	E138K	F227L/V106A	RES056	(μM)[b]
7	3-COMe-Ph	0.041±0.005	0.36±0.10	2.1±0.15	25.7±0.7	>81.3	2.2±0.02	3.6±0.8	>81.3	81.3±31.6
8	-CH_2OH	**0.006±0.002**	**0.017±0.008**	**0.084±0.015**	**0.13±0.011**	**>6.3**	**0.14±0.01**	**0.22±0.15**	**>6.3**	**6.3±5.8**
9	4-SO_2NH_2-Ph	0.014±0.008	0.048±0.015	0.33±0.12	0.45±0.12	>5.9	0.12±0.00	0.74±0.29	>5.9	5.9±2.3
10	4-Cl-Ph	0.13±0.06	0.55±0.05	3.6±0.6	17.3±5.4	>67.3	3.2±0.3	3.6±1.8	>67.3	67.3±15.7
11	3-Cl-Ph	0.30±0.15	3.5±0.3	10.2±2.2	15.1±1.3	>103.0	3.9±0.2	20.2±7.6	>103.0	103.0±15.1
12	pyridin-3-yl	0.019±0.009	0.076±0.050	0.22±0.034	0.60±0.05	>6.6	0.17±0.02	0.40±0.17	>6.6	6.6±3.0
13	pyridin-4-yl	0.017±0.005	0.034±0.010	0.28±0.02	0.57±0.07	≥4.6	0.10±0.01	0.21	>9.8	9.8±3.5
14	4-$CONH_2$-Ph	0.012±0.005	0.026±0.002	0.13±0.10	0.29±0.11	≥3.2	0.10±0.02	0.30±0.05	≥5.2	8.8±5.4
15	4-SO_2Me-Ph	0.020±0.01	0.086±0.002	0.44±0.03	0.55±0.02	6.0±1.1	0.14±0.01	0.41±0.08	≥6.4	14.6±8.1
16	pyridin-3-yl	0.012±0.008	0.034±0.004	0.22±0.06	0.56±0.06	4.8±0.8	0.14±0.10	0.39±0.19	≥5.9	6.9±5.2
17	pyridin-4-yl	0.016±0.010	0.048±0.009	0.24±0.04	0.73	5.1±0.2	0.10±0.00	0.43±0.17	>20.8	20.8±3.0
18	4-methyl-2H-1,2,4-triazol -3(4H)-one 3-yl	**0.009±0.004**	**0.049±0.007**	**0.18±0.02**	**0.20±0.05**	**0.84±0.21**	**0.043±0.8**	**0.27±0.09**	**>14.0**	**14.0±4.8**
19	4-SO_2NH_2-Ph	0.013±0.007	0.083±0.065	0.29±0.05	0.44±0.02	3.4±0.4	0.18±0.02	0.44±0.16	≥5.4	7.7±5.7
20	4-$CONH_2$-Ph	0.011±0.008	0.029±0.005	0.12±0.01	0.29±0.09	4.7±1.6	0.086±0.00	0.17±0.09	**4.4±1.5**	6.2±2.1
21	thiophene-2-yl	0.022±0.013	0.031±0.006	0.23±0.04	0.87±0.15	>90.6	0.65±0.07	0.35±0.06	>90.6	90.6±21.0
22	thiophene-3-yl	0.031±0.015	0.13±0.08	0.73±0.04	9.4±11.0	>49.6	0.81±0.07	1.9±0.8	>49.6	49.6±18.7
23	4-CF_3-Ph	0.17±0.05	1.1±0.05	5.1±0.7	>16.0	>16.0	4.3±0.8	7.4±0.7	>16.0	16.0±3.9
24	furan-3-yl	0.018±0.010	0.032±0.004	0.21±0.00	0.61±0.15	>162.6	0.13±0.03	0.19±0.01	>162.6	162.6±44.5
25	4-NO_2-Ph	0.62±0.43	≥19.1	≥31.9	>57.3	>57.3	≥38.2	>57.3	>57.3	57.3±49.1
26	-CH_2OH	0.032±0.020	0.11±0.03	0.32±0.10	0.56±0.02	>6.7	0.30±0.12	0.62	>6.7	6.7±5.6
27	4-$CONH_2$-Ph	0.024±0.008	0.11±0.01	0.49±0.10	0.69±0.08	>3.4	0.11±0.02	0.76±0.08	>3.4	3.4±0.5
28	3-F-Ph	0.18±0.16	0.49±0.14	1.5±0.07	4.6±0.3	>61.3	0.33±0.16	4.2±0.3	>61.3	61.3±23.4
29	3-CN-Ph	0.14±0.09	0.96±0.31	3.1±0.05	3.4±0.4	≥20.7	0.13±0.00	3.3±0.05	>34.8	>34.8
30	CH_2COOEt	0.027±0.012	0.29±0.21	0.55±0.41	0.75±0.16	4.8±0.5	0.20±0.05	1.7±1.6	>19.2	19.2±2.9
NVP		0.12±0.07	0.71±0.45	3.6±2.4	3.8±2.6	4.4±2.5	0.16±0.11	3.5±2.7	2.2±0.8	>15.0
DLV		0.024±0.024	3.5±3.0	2.5±1.8	1.9±1.4	0.55±0.39	0.070±0.06	2.6±3.0	≥37.0	>43.8
EFV		0.003±0.002	0.057±0.044	0.098±0.057	0.005±0.002	0.092±0.06	0.005±0.001	0.076±0.06	0.11±0.06	>6.3
ETV		0.003±0.000	0.009±0.006	0.003±0.007	0.014±0.006	0.015±0.06	0.011±0.007	0.015±0.006	0.034±0.0	2.2±0.0

[a]EC_{50}: concentration of compound required to achieve 50% protection of MT-4 cell cultures against HIV-1-induced cytotoxicity, as determined by the MTT method.

[b]CC_{50}: concentration required to reduce the viability of mock-infected cell cultures by 50%, as

determined by the MTT method.

[c]SI: selectivity index, the ratio of CC_{50}/EC_{50}.

Table 1 (Continued). Activity against HIV-1 strains, cytotoxicity and selectivity index in MT-4 cells.

Compd.	SI[c]							
	IIIB	**L100I**	**K103N**	**Y181C**	**Y188L**	**E138K**	**F227L/V106A**	**RES056**
7	2004	221	40	3	<1	37	23	<1
8	1005	368	74	48	<1	46	28	<1
9	411	123	18	13	<1	49	8	<1
10	513	121	19	4	<1	21	19	<1
11	346	29	10	7	<1	26	5	<1
12	338	88	30	11	≤1	37	17	<1
13	568	282	36	17	≤2	96	47	<1
14	728	348	66	30	≤3	86	29	≤2
15	746	169	34	27	104	104	35	≤2
16	589	209	30	13	49	49	18	≤1
17	1276	436	84	29	213	213	48	<1
18	1476	289	76	73	17	320	54	<1
19	592	94	26	17	2	43	18	≤1
20	576	208	50	21	1	72	37	1
21	3951	2951	382	104	<1	140	263	<1
22	1610	372	67	5	<1	61	25	<1
23	93	14	3	<1	<1	4	2	<1
24	9391	4958	792	265	<1	1267	834	<1
25	93	≤3	≤2	<1	<1	≤2	<1	<1
26	205	59	21	12	<1	22	11	<1
27	147	31	7	5	<1	31	4	<1
28	338	123	42	13	<1	181	14	<1
29	>257	>36	>11	>10	≤2	>263	>10	X
30	740	67	34	26	4	98	11	<1
NVP	>127	>21	>4	>4	>3	>95	>4	>7
DLV	1879	13	18	23	81	634	17	X
EFV	>2372	>110	>64	>1282	>68	>1356	>82	>55
ETV	1163	503	1361	327	299	429	282	131

Table 2. Inhibitory activity of compounds **18**, **30**, NVP and ETV against HIV-1 RT.

Compd.	**18**	**30**	**NVP**	**ETV**
IC_{50} (μM)[a]	7.0	10.1	2.8	1.1

[a]IC_{50}: inhibitory concentration of test compound required to inhibit biotin deoxyuridine triphosphate (biotin-dUTP) incorporation into HIV-1 (WT) RT by 50%.

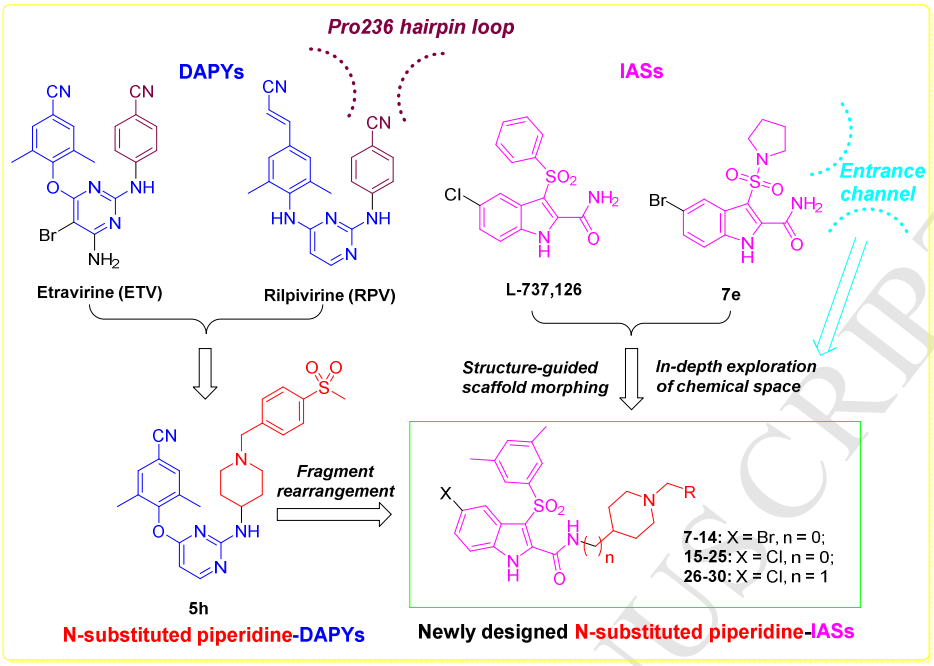

Figure 1. The structures of representative DAPYs (Etravirine, Rilpivirine and 5h) and IASs (L-737,126, 7e), and the newly designed N-substituted piperidine-IASs via the combination of structure-guided scaffold morphing and fragment rearrangement approaches.

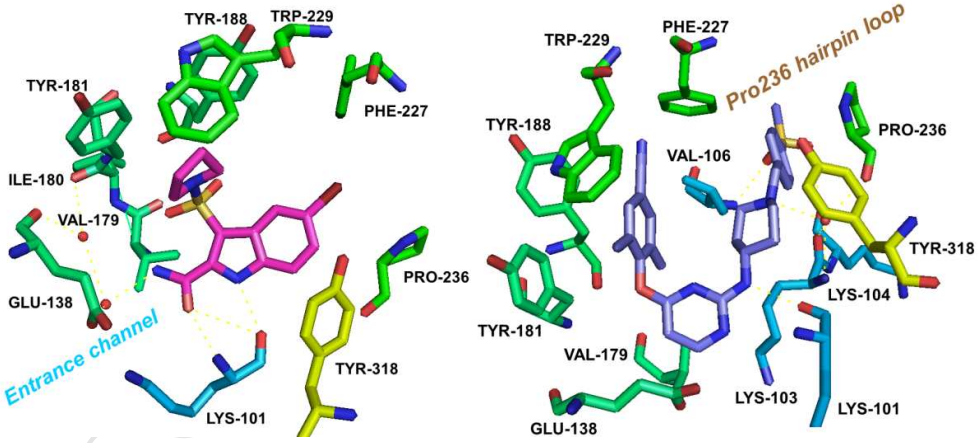

Figure 2. Schematic diagram of the binding modes of IASs and DAPYs with NNIBP: (a) HIV RT in complex with inhibitor **7e** (pink) (PDB code: 2RF2); (b) HIV RT in complex with inhibitor **5h** (dark blue) (PDB code: 3M8Q). These figures was generated using PyMOL (www.pymol.org). Residues important for binding are shown as sticks. Hydrogen bonds are indicated by yellow dashes.

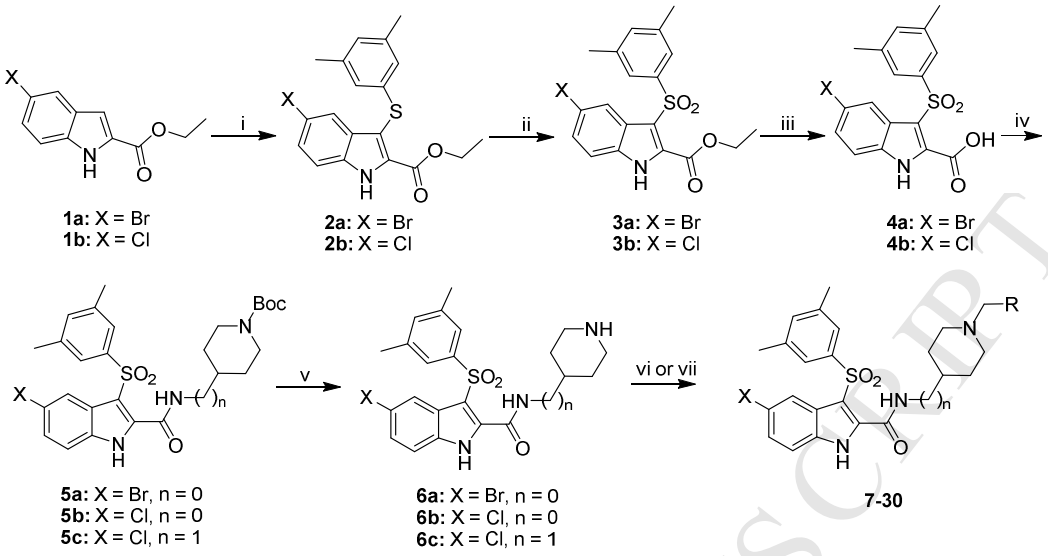

Scheme 1. Reagents and conditions: (i) 3,5-dimethylbenzenethiol, Selettflour^{TM}, MeCN; (ii) M-chloroperoxybenzoic acid, CH_2Cl_2, 0°C; (iii) LiOH, H_2O, THF, 50°C; (iv) 1-Boc-4-(aminomethyl)-piperidine or 1-Boc-4-aminopiperidine, HATU, EDC·HCl, Et_3N, DMF; (v) CF_3COOH, CH_2Cl_2; (vi) K_2CO_3, DMF, substituted benzyl; (vii) substituted-aldehyde AcOH, $NaBH_3CN$, THF/MeCN.

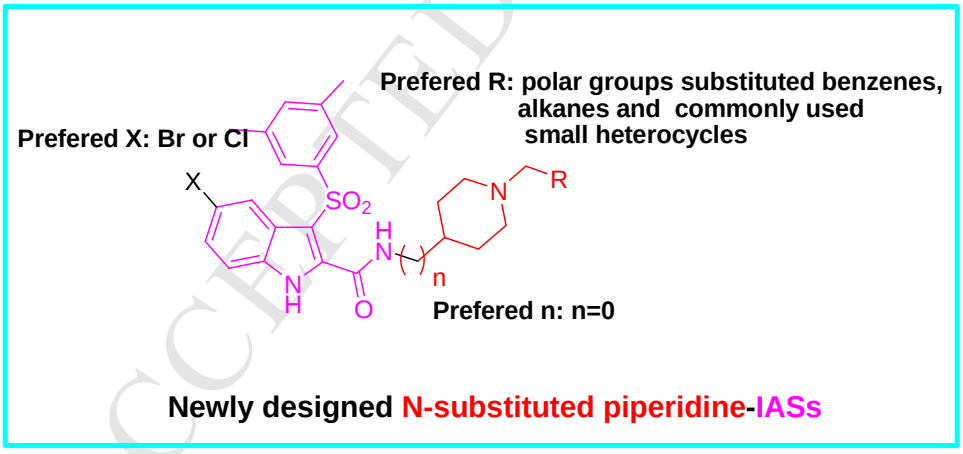

Figure 3. A illustrative figure of the SARs

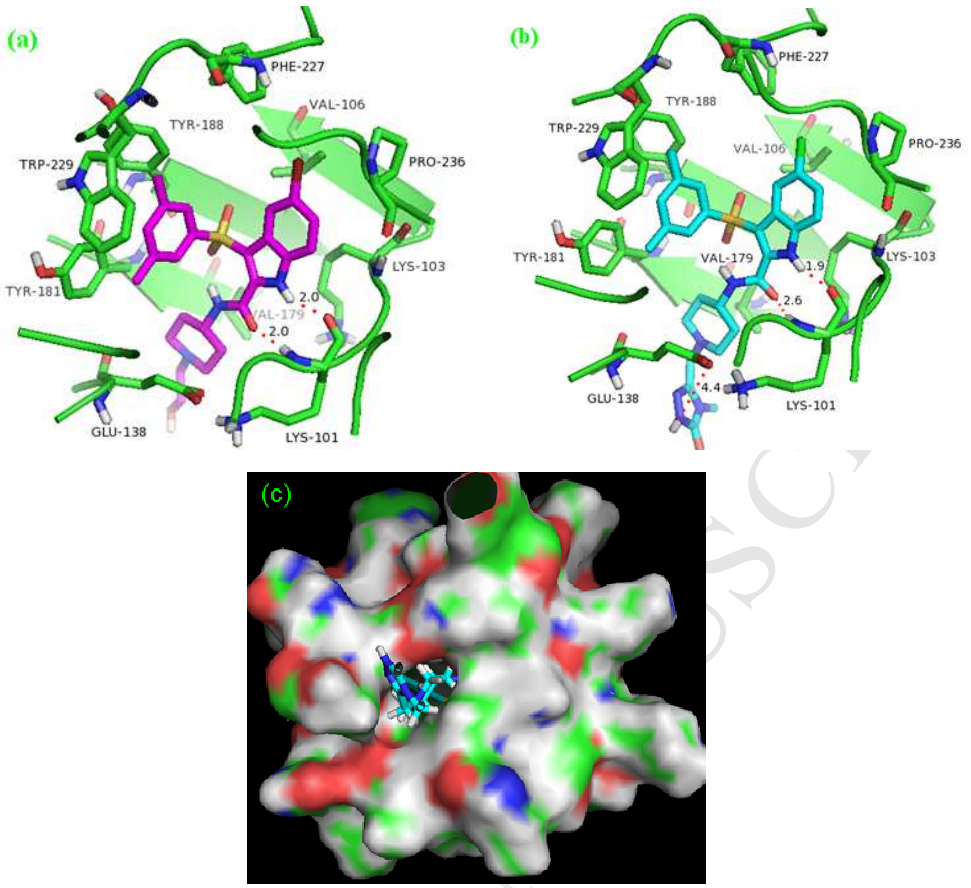

Figure 4. Predicted binding modes of novel IASs in the allosteric site of HIV-1 WT RT (PDB code: 2rf2): (a) Ribbon model of the **8** binding; (b) Ribbon model of the **18** binding (c) Surface presentation of **18** located toward a solvent exposure region. Hydrogen bonds are indicated with dashed lines in red, and hydrogen atoms are omitted for clarity.

Highlight:

Novel IASs bearing *N*-substituted piperidine at indole-2-carboxamide were designed

New IASs have EC_{50} values ranging from 0.62 μM to 0.006 μM against WT HIV-1

Compounds **8** (EC_{50} = 6 nM) and **18** (EC_{50} = 9 nM) were the most active derivatives

Compounds **8** and **18** also displayed outstanding potency against some HIV-1 mutants

SARs and molecular modeling studies were discussed in detail